Received: 22 February 2023 | Accepted: 28 April 2023

DOI: 10.1111/1751-7915.14272

MICROBIAL BIOTECHNOLOGY Applied Microbiology International

RESEARCH ARTICLE

Nanohaloarchaea as beneficiaries of xylan degradation by haloarchaea

Violetta La Cono[1] | Enzo Messina[2] | Oleg Reva[3] | Francesco Smedile[1] | Gina La Spada[1] | Francesca Crisafi[1] | Laura Marturano[1] | Noa Miguez[4] | Manuel Ferrer[4] | Elena A. Selivanova[5] | Olga V. Golyshina[6] | Peter N. Golyshin[6] | Manfred Rohde[7] | Mart Krupovic[8] | Alexander Y. Merkel[9] | Dimitry Y. Sorokin[9,10] | John E. Hallsworth[11] | Michail M. Yakimov[1]

[1]Institute of Polar Research, ISP-CNR, Messina, Italy

[2]National Council of Research, CNR, Rome, Italy

[3]Department of Biochemistry, Genetics and Microbiology, Faculty of Natural and Agricultural Sciences, Centre for Bioinformatics and Computational Biology, University of Pretoria, Pretoria, South Africa

[4]Instituto de Catalisis y Petroleoquimica (ICP), CSIC, Madrid, Spain

[5]Institute for Cellular and Intracellular Symbiosis, Ural Branch, Russian Academy of Sciences, Orenburg, Russia

[6]School of Biological Sciences, Bangor University, Bangor, UK

[7]Central Facility for Microbiology, Helmholtz Centre for Infection Research, Braunschweig, Germany

[8]Institut Pasteur, Université Paris Cité, Archaeal Virology Unit, Paris, France

[9]Winogradsky Institute of Microbiology, Research Centre of Biotechnology, Russian Academy of Sciences, Moscow, Russia

[10]Department of Biotechnology, Delft University of Technology, Delft, The Netherlands

[11]Institute for Global Food Security, School of Biological Sciences, Queen's University Belfast, Northern Ireland, UK

Correspondence
Michail M. Yakimov, Institute of Polar Research, ISP-CNR, Spianata San Raineri 86, 98122 Messina, Italy.
Email: mikhail.iakimov@cnr.it

Funding information
Agence Nationale de la Recherche, Grant/Award Number: ANR-20-CE20-0009; Centre for Environmental Biotechnology Project, partly funded by the European Regional Development Fund via the Welsh Assembly Government; European Union ("NextGen-eration EU/PRTR"); H2020 Food, Grant/Award Number: INMARE Project (Contract 2634486) and FUTURENZYMES Project (Contract 101000327); Ministerio de Ciencia e Innovación, Agencia Estatal de Investigación (AEI) (Digital Object Identifier 10.13039/501100011033, Grant/Award Number: PID2020-112758RB-I00, PDC2021-121534-I00 and TED2; SYAM-Gravitation Program of the Dutch Ministry of Education, Culture and Science, Grant/Award Number: 24002002

Abstract

Climate change, desertification, salinisation of soils and the changing hydrology of the Earth are creating or modifying microbial habitats at all scales including the oceans, saline groundwaters and brine lakes. In environments that are saline or hypersaline, the biodegradation of recalcitrant plant and animal polysaccharides can be inhibited by salt-induced microbial stress and/or by limitation of the metabolic capabilities of halophilic microbes. We recently demonstrated that the chitinolytic haloarchaeon *Halomicrobium* can serve as the host for an ectosymbiont, nanohaloarchaeon '*Candidatus* Nanohalobium constans'. Here, we consider whether nanohaloarchaea can benefit from the haloarchaea-mediated degradation of xylan, a major hemicellulose component of wood. Using samples of natural evaporitic brines and anthropogenic solar salterns, we describe genome-inferred trophic relations in two extremely halophilic xylan-degrading three-member consortia. We succeeded in genome assembly and closure for all members of both xylan-degrading cultures and elucidated the respective food chains within these consortia. We provide evidence that ectosymbiontic nanohaloarchaea is an active ecophysiological component of extremely halophilic xylan-degrading communities (although *by proxy*) in hypersaline environments. In each consortium, nanohaloarchaea occur as ectosymbionts of *Haloferax*, which in turn act as scavenger

of oligosaccharides produced by xylan-hydrolysing *Halorhabdus*. We further obtained and characterised the nanohaloarchaea–host associations using microscopy, multi-omics and cultivation approaches. The current study also doubled culturable nanohaloarchaeal symbionts and demonstrated that these enigmatic nano-sized archaea can be readily isolated in binary co-cultures using an appropriate enrichment strategy. We discuss the implications of xylan degradation by halophiles in biotechnology and for the United Nation's Sustainable Development Goals.

INTRODUCTION

Plant biomass must be ultimately degraded to avert a build-up of dead material and ensure the functioning of nutrient cycles at global, ecosystem and microbial community scales. However, many plant polysaccharides are recalcitrant, including cellulose, xylan and other hemicelluloses. Under conditions and in environments that are highly stressful or extreme, saprotrophic degradation and other microbial activities can be severely inhibited. Furthermore, the genomes of individual microorganisms may not encode the full enzymatic repertoire required to saprotrophically break down polysaccharides. Microbes unable to fully catabolise polysaccharides include some psychrotolerant microbes in cold locations and extremely halophilic microbes that are found in salt-saturated brines (Hallsworth, 2019; Li et al., 2022).

Most of the waters on Earth contain salt(s), including those of the oceans, some aquifers, saline and brine lakes and those in otherwise frozen environments (Boetius & Joye, 2009; Drever, 1988; Lee et al., 2018; Saccò et al., 2021). Plant necromass—including wood and its breakdown products—can therefore end up immersed in salt-containing water that can be hostile to those microbes that are neither halotolerant nor halophilic. Furthermore, brines can be hostile even for halophilic or polyextremophilic microorganisms and are in some cases effectively sterile (Belilla et al., 2019; Benison et al., 2021; Cavalazzi et al., 2019; Hallsworth, 2019; Hallsworth et al., 2007; Martínez et al., 2021). It is in part for this reason, halophilic microbes—and their ability/inability to subsist via saprotrophic nutrition—are pertinent to a number of the Sustainable Development Goals (SDGs) of the United Nations (Sachs et al., 2022) see also below.

Extremely halophilic archaea of the class *Halobacteria* (phylum *Euryarchaeota*) form dense blooms in inland salt-saturated lakes and the final evaporation pools of marine solar salterns. Most of the laboratory-cultivated haloarchaea species are aerobic heterotrophs that are grown as pure cultures on simple soluble organic monomers or amino acid-rich substrates including yeast extract and various peptones. Although some haloarchaea are able to hydrolyse high molecular weight polymeric substances such as starch and proteins, there are only a few indications of their abilities to degrade and consume cellulose, chitin and hemicelluloses, the three most abundant groups of polysaccharides on Earth, including hypersaline habitats (Figure S1). Thus, the mineralisation of these insoluble polymers in natural hypersaline habitats has previously been attributed almost exclusively to halophilic bacteria (Andrei et al., 2012; Oren, 2013). However, recent studies have shown that some haloarchaea originating from brines and sediments of geographically distant hypersaline lakes can be enriched and isolated using insoluble forms of either natural cellulose or chitin as sole growth substrates (La Cono et al., 2020; Sorokin et al., 2015, 2019). In addition, they seem to play a key role in the primary decomposition of other insoluble polysaccharides in salt-saturated environments (Sorokin et al., 2022).

Whereas cellulose and chitin are almost exclusively composed of glucose and *N*-acetyl glucosamine, respectively, hemicelluloses are mostly heteropolymers composed of diverse sugars in both their main and side chains. In this respect, xylans are typical heteropolysaccharides and are the major hemicellulose type of many plant materials. They consist of a homopolymer backbone chain of 1,4-linked β-D-xylopyranose units and side chains that may contain arabinose, galactose, glucuronic acid (or its 4-*O*-methyl ether) and acetic, ferulic and/or *p*-coumaric acids. Based on such structural and compositional complexity, the complete enzymatic hydrolysis of xylans requires a complex set of hydrolytic enzymes. They include endo-β-1,4-xylanase (glycosyl hydrolases of families GH10 and GH11; EC 3.2.1.8), β-xylosidase (GH16 and GH43 families; EC 3.2.1.37), and several accessory enzymes such as acetylxylan esterase (carboxyl esterase of CE6 family; EC 3.1.1.72), α-L-arabinofuranosidase (GH51 family; EC 3.2.1.55), α-D-glucuronidase (GH67 family; EC 3.2.1.139), α-D-galactosidase (GH97 family; EC 3.2.1.20) and feruloyl esterase (EC 3.1.1.73), which are necessary for hydrolysing xylose substitutions (side chains).

As we mentioned above, there is little evidence documented of xylan degradation in hypersaline habitats by haloarchaea. The first study reported that the extremely halophilic archaeon *Halorhabdus utahensis* (from the Great Salt Lake, Utah, USA) could grow on birchwood xylan and exhibited both extracellular β-xylanase and

β-xylosidase activities (Wainø & Ingvorsen, 2003). The genome analysis and functional assays of another species of this genus, *Hrb. thiamatea*, isolated from deep-sea hypersaline anoxic basins of the Red Sea and the Mediterranean Sea, suggested an entire enzymatic repertoire for xylan depolymerisation (Werner et al., 2014). Recently, the xylanase activity has also been demonstrated in some isolates of the genera Natrinema (Karray et al., 2018), *Halococcus* and *Halorubrum* (Malik & Furtado, 2019). However, all these studies were originally based either on measurements of enzymatic activity or on genomic information and not on the enrichment of the organism in culture to confirm and measure the degradation of xylan provided as the sole source of carbon and energy. Yet, it remains unclear whether haloarchaea readily degrade xylan when this substrate is present in their natural hypersaline habitats.

We recently demonstrated that chitinolytic haloarchaeon *Halomicrobium* sp. LC1Hm may coexist in association with the nano-sized ectosymbiont *Ca*. Nanohalobium constans LC1Nh, a member of the candidate phylum Nanohaloarchaeota (La Cono et al., 2020; Messina et al., 2021). These extremely halophilic archaea—with diminutive cells and reduced genomes—were first detected during cultivation-independent studies of the biota of an African alkaline saltern (Grant et al., 1999). Modern cultivation-independent studies have shown that nanohaloarchaea are found often in large numbers (>10^6 cells mL^{-1}) in natural salt lakes, sea saltern brines and deep-sea hypersaline anoxic lakes around the world (Crits-Christoph et al., 2016; Di Meglio et al., 2016; Feng et al., 2021; Ghai et al., 2011; Gomariz et al., 2015; Mora-Ruiz et al., 2018; Narasingarao et al., 2012; Podell et al., 2014; Selivanova et al., 2018). Our cultivation experiments revealed a remarkable mutualism of the *Ca*. Nanohalobium–*Halomicrobium* association, namely the nanohaloarchaeon's ability to hydrolyse glycogen and starch to glucose (a metabolic feature not present in the host), enables the growth of *Halomicrobium* sp. LC1Hm in the absence of chitin (La Cono et al., 2020). We also then suggested that similar enrichment approaches using different polysaccharides as the sole source of carbon and energy will bring other hitherto unculturable Nanohaloarchaeota taxa into culture (La Cono et al., 2020).

Using xylan as the only growth substrate and source of energy, we report here a detailed characterisation of two xylanolytic consortia that were obtained, respectively, from brines of the natural hypersaline Sol-Iletsk lakes Razval and Dunino (Russia) and from brine and sediments of the Saltern of Margherita di Savoia crystalliser pond (Italy), Europe's largest marine saltern. Despite the fact that the resulting consortia were obtained from geographically distant hypersaline ecosystems, they were very similar to each other. In addition to the xylanolytic haloarchaeon *Halorhabdus*, both consortia also consisted of two other members, namely, ectosymbontic nanohaloarchaea associated with a xylose-consuming haloarchaeal host, *Haloferax*. Besides axenic cultures of haloarchaea, the two corresponding binary associations of nanohaloarchaea, dubbed *Candidatus* Nanohalococcus occultus SVXNc (Nanohalococcus SVXNc for short) and Ca. Nanohalovita haloferacivicina BNXNv (Nanohalovita BNXNv for short) with their hosts were obtained, stably cultivated and characterised in growth experiments using electron microscopy, genome sequencing, transcriptomics, proteomics and metabolomics.

EXPERIMENTAL PROCEDURES

Sample collection and initial treatments

Samples of near-bottom brine (50 mL) and surface sediment (from a 2-cm depth and mainly composed of salt crystals) were taken from two pH-neutral hypersaline Na^+, K^+, Cl^- (total salinity 300 $g\,L^{-1}$; pH 7.1–7.5) lakes *Razval* and *Dunino* (Sol-Iletsk region, Russia: 51.151° N, 55.003° E) in June 2019, and from the crystalliser pond *Cappella* (total salinity 346 $g\,L^{-1}$; pH 7.27) of the marine solar saltern Margherita di Savoia (south Italy: 41.3782° N, 16.1301° E) also in June 2019. The slurry samples were extruded into a sterile Schott flask (50 mL), sealed (without air bubbles), transported to the laboratory and stored at 10°C until use. The sediment slurries from the two Sol-Iletsk lakes were mixed in equal proportions to produce a combined inoculum. For initial enrichments, this combined sediment/brine inoculum (10% v/v; see below) was added to the liquid mineral medium supplemented with xylan (see below). The same procedure was carried out for the sample from crystalliser pond *Cappella*.

Enrichment and isolation of an axenic haloarchaeal cultures from xylanolytic consortia

Based on knowledge of the successful isolation and maintenance of the *Ca*. Nanohalobium–*Halomicrobium* co-culture (La Cono et al., 2020), the same Laguna Chitin liquid mineral medium (total salinity 240 $g\,L^{-1}$) was used. The pH was adjusted to 7.4 by the addition of 1 M KOH. After sterilisation (121°C, 20 min) and cooling, the medium was supplemented with 1 $mL\,L^{-1}$ acidic trace metal solution (Pfennig & Lippert, 1966), 1 $mL\,L^{-1}$ vitamin mix (Pfennig & Lippert, 1966) and 100 $mg\,L^{-1}$ yeast extract. Xylan from beechwood (Megazyme, catalogue number P-XYLNBE-10G) was sterilised separately by autoclaving and then added at a final concentration of 2 $g\,L^{-1}$, to serve as the growth substrate. The bacteria-specific antibiotics vancomycin and streptomycin were

added (100 mg L^{-1} of each, final concentration) to prevent the growth of any halophilic bacteria.

Enrichment cultures, *S*ol-Iletsk *V*arious *X*ylan (SVX) and *B*ari *N*ew *X*ylan (BNX) were initiated by mixing 10 mL of the appropriate slurry with 90 mL of sterile Laguna Chitin liquid medium, supplemented with xylan. Both these enrichments were incubated at 40°C in tightly sealed 120-mL glass serum vials in the dark and without shaking for 2–3 months. The isolation strategy for axenic xylanolytic cultures consisted of several rounds of decimal-dilution transfers (each inoculation to fresh Laguna Chitin liquid medium being a 10-fold dilution by adding 10% by volume of culture to 90% by volume fresh medium) to obtain active xylanolytic sediment-free enrichments, followed by a three-fold repetition of serial dilution-to-extinction (Figure S2). In each case, the lowest dilution at which growth occurred was determined according to growth in the Laguna Chitin liquid medium that had been supplemented with xylan only. After the appearance of an intense red colour, 5 μL of the grown culture was diluted in 5 mL of Laguna Chitin liquid mineral medium, and then 50 μL of the resulting dilution was spread on Laguna Chitin agar (1.5%, w/v) plates, respectively, supplemented with either xylan (2 g L^{-1}) or D-xylose (2 g L^{-1}, Sigma Alrdich, catalogue number X0200000). These substances were used to achieve two goals: to obtain single colonies of xylanolytic haloarchaea (xylan) and to assess the level of satellite haloarchaea (D-xylose), which are incapable of xylan degradation but able to grow on its monomer, respectively. The grown colonies were picked and used to inoculate the Laguna Chitin liquid medium that had been supplemented with xylan (2 g L^{-1}). Finally, the purity of isolates was checked by 16S rRNA gene cloning and sequencing of at least 16 clones from each library.

Enrichment and isolation of binary nanohaloarchaeon–Haloarchaeon co-culture

Using primers specific for nanohaloarchaea (La Cono et al., 2020), their presence of the latter was already confirmed in decimal dilutions (see above), warranted bringing them to culture following the same experimental design applied for isolation of the *Ca*. Nanohalobium–*Halomicrobium* co-culture (La Cono et al., 2020). After confirmation by PCR, for each sample, the last dilutions positive for nanohaloarchaea were passed three times through a 0.45-μm pore syringe filter (Sartorius Stedim Biotech) (Figure S2). For each sample, the third (final) filtrate was additionally checked using a euryarchaea-specific PCR to verify the purity of nanohaloarchaeon cell suspension. Thereafter, and using triplicates, 1 mL filtrate was mixed with 10 mL Laguna Chitin liquid medium that has been supplemented with D-xylose (2 g L^{-1}) and 1 mL of fresh (72 h - grown) axenic culture of either *Halorhabdus* or *Haloferax* was added. The co-cultures thus obtained were grown statically (to maintain microaerobic conditions) in 15 mL Falcon tubes at 40°C for 2–3 weeks and the increase in nanohaloarchaeal cell number was monitored daily by nanohaloarchaea-specific PCR.

Chemical analyses

Oligosaccharides were analysed by high-performance anion-exchange chromatography with pulsed amperometric detection (HPAEC-PAD). For this purpose, culture supernatants (300-μL aliquots) were firstly mixed with absolute ethanol to a final concentration of ethanol 70% (v/v) to precipitate any protein and polysaccharide material. The samples were then centrifuged (10,000 *g*, 5 min) and then filtered with 0.45-μm nylon filters (Cosela S.L.). The analysis was carried out at 30°C by HPAEC-PAD, Dionex ICS3000 system, an anion-exchange CarboPack PA-100 column (4 mm × 250 mm) connected to a CarboPac PA-100 guard column (4 m × 50 mm), and an autosampler (model AS-HV). The analysis was performed at a flow rate of 0.5 mL min^{-1} and the mobile phase contained 10 mM NaOH from start to end, while two gradients were performed with AcONa. The first was an 80 min gradient from 0 to 60 mM AcONa, and the second was from 60 to 160 mM in 20 min. Finally, the column was equilibrated back to the initial conditions. Eluents were degassed by flushing with helium and peaks were analysed using Chromeleon software. The identification of some of the reaction products was performed compared to standards (all provided by Merck Life Science S.L.U.), which include, glucose-based saccharides (e.g., glucose, maltose, maltotriose) and xylo-oligosaccharides (e.g., xylose, xylobiose, xylotriose).

Two cultures, namely the axenic culture of *Hfx. lucertense* SVX82 and the binary culture of *Hfx. lucertense* SVX82 + Ca. Nanohalococcus occultus SVXNc (each in two replicates), were grown statically in the LC medium containing xylose (200 mM) at 40°C for 120 h. Cell lysis was performed as previously described (La Cono et al., 2020; Sorokin et al., 2021). To determine the intracellular concentration of glucose-6-phosphate, the glucose-6-phosphate assay kit (Merck Life Science S.L.U.) was used. To calculate the intracellular concentration of glucose-6-phosphate (mM), it was assumed that 1.67 g of wet cells contain 1 mL of cell volume (Conway & Downey, 1950; Sáez & Lagunas, 1976). Based on this, after weighing, the volume of cells was calculated as the total volume of extracted intracellular material. We were aware that the presence of nanohaloarchaea in a binary culture could affect the final (calculated) concentration of intracellular glucose-6-phosphate (mM) and their possible total volume was also taken into consideration. Given that both *Hfx.*

lucertense SVX82 and Ca. Nanohalococcus occultus SVXNc are coccoid, and the average host cell size is about 2 μm, and nanohaloarchaeal cell is about 0.25 μm, the volume of an individual host cell (4.19 μm) is 300 times larger than the volume of a single nanohaloarchaeal cell (0.014 μm).

Microbial enumeration by serial dilutions/plating and quantitative PCR

The *Halorhabdus*–*Haloferax*–Ca. Nanohalococcus three-membered culture was grown in hypersaline LC mineral medium supplemented with vitamins, yeast extract, antibiotics and xylan (2 g L^{-1}), while both the *Haloferax*–Ca. Nanohalococcus co-culture and the *Hfx, lucertense* SVX82 axenic culture were grown in the same medium supplemented with D-xylose (200 mM). All cultures were maintained (in triplicates) at pH 7.0 at 40°C, and their growth was observed over a 240 h period. Quantitative assessment of haloarchaea and nanohaloarchaeon in both the three-membered and binary cultures was carried out using two different enumeration methods. The quantitative PCR (qPCR) method was used to determine the relative cell densities of Ca. Nanohalococcus as previously described (La Cono et al., 2020). However, many species of the genus *Haloferax* are known to be highly polyploid, containing up to 20 copies of the major chromosome per cell (Lange et al., 2011). To avoid possible inconsistencies in enumeration results using a DNA-based qPCR method, the classical serial dilution/plating approach was applied instead. At regular intervals, grown culture (100 μL) was diluted to 10^{-8}–10^{-9} and 20–50 μL of these 10-fold serial dilutions were plated as five spatially separated droplets on LC agar (1.5%, w/v) plates supplemented with D-xylose (200 mM). Due to the significant difference in colony morphology between *Halorhabdus* (small, rigid red colonies) and *Haloferax* (significantly larger, less intense teardrop-like colonies), the colonies originated on the Petri plates from a single cell could be readily identified. These were counted to estimate the number of colony-forming units per millilitre (cfu) in a given suspension, represented as cfu mL^{-1} or cells mL^{-1}.

Field emission scanning electron microscopy (FESEM)

The grown cells were fixed with 2% (v/v, final concentration) freshly prepared paraformaldehyde. The fixative was removed by washing twice with LC mineral medium. Following that, a final fixation with aqueous osmium tetroxide was carried out (four parts LC mineral medium and one part 5% [w/v] aqueous osmium tetroxide) for 30 min at 25°C. The fixed material was then washed with LC mineral medium and placed onto poly-L-lysine-coated coverslips for 10 min, followed by treatment with 1% (v/v) glutaraldehyde to cross-link microbes with poly-L-lysine coating. This step prevents cells from being washed away during the dehydration and critical point drying of the attached microorganisms. Dehydrating was achieved using a series of acetone–water mixtures and pure acetone (10, 30, 50, 70, 90, and 100% [v/v] acetone) on ice for 10 min for each step. Once in the 100% acetone, samples were allowed to reach 25°C (evaporation of acetone has cooled the sample), replenishing with fresh 100% acetone. Samples were then subjected to critical point drying with liquid CO_2 (CPD 030, Bal-Tec, Liechtenstein). Dried samples were covered with a gold–palladium film by sputter coating (SCD 500 Bal-Tec, Liechtenstein) before examination in a field emission scanning electron microscope Zeiss Merlin (Carl Zeiss, Oberkochen) using the Everhart Thornley SE-detector and the in-lens secondary electron detector in a 50:50 ratio with an acceleration voltage of 5 kV.

Ultra-thin sections and transmission electron microscopy (TEM)

Glutaraldehyde-fixed samples (see above) were washed twice with LC mineral medium and fixed with 1% (w/v) aqueous osmium (final concentration) for 1 h at 25°C. Samples were then embedded into hot aqueous agar solution 2% (w/v), solidified agar was cut into small cubes and dehydrated with a graded series of ethanol–water mixtures and pure ethanol (10, 30, 50, 70, 90 and 100% [v/v] ethanol) for 30 minutes at each step. The 100% ethanol step was repeated twice before the samples were infiltrated with 100% ethanol and LRWhite resin (50:50 ratio) for 8 h followed by one part 100% ethanol and two parts LRWhite resin for 24 h hours and subsequently infiltrated with pure LRWhite resin with two changes over 2 days. The next day 1 μL starter was added to 10 mL LRWhite resin, stirred and resin was put into 0.5 mL gelatin capsules. The samples were placed into the tip of the capsules, followed by polymerisation for 2 days at 50°C. Ultrathin sections were cut with a diamond knife and these sections were counter-stained with 4% (w/v) aqueous uranyl acetate for 3 min. Samples were examined in a TEM910 transmission electron microscope (Carl Zeiss) at an acceleration voltage of 80 kV. Images were taken at calibrated magnifications, recorded digitally with a Slow-Scan CCD Camera (ProScan, 1024×1024) with ITEM Software (Olympus Soft Imaging Solutions), and the contrast and brightness were adjusted with Adobe Photoshop CS5. For negative staining of whole cells for TEM, thin carbon support films were prepared by sublimation of a carbon thread onto a freshly cleaved mica surface. Osmium-fixed cells were adsorbed onto the

carbon film and negatively stained with 0.5% (w/v) uranyl acetate solution, pH 5.0, according to the method of Valentine et al. (1968). Samples were examined in a TEM 910 transmission electron microscope (see above).

Genome sequencing and assembly, phylogenetic and phylogenomic analyses

Whole-genome shotgun sequencing of the three-membered, binary and axenic cultures was done by FISABIO using the Illumina® MiSeq System platform with 2 × 300 bp short insert paired-end libraries (MiSeq Reagent Kit v3). FISABIO also performed the quality assessment and the sequence joining (forward R1 and reverse R2). Quality assessment was performed with the PRINSEQ-lite program (Schmieder & Edwards, 2011) using the following parameters: Min_length:50 bp trim_qual_right:30 bp trim_qual_typ:mean, trim_qual_window:20 bp. Forward and reverse reads were joined by the FLASH program (Magoč & Salzberg, 2011) applying default parameters. All six genomes were assembled as single circular chromosomes and, in case of *Hfx. lucertense* SVX82 and BNX82, three and four plasmids, respectively, and analysed as described previously (La Cono et al., 2020; Sorokin et al., 2021). The genome statistics are given in Tables S1 and S2.

For genome-based phylogenetic reconstructions, 122 archaeal single-copy conservative marker genes were used as described previously (Parks et al., 2020; Rinke et al., 2021). The genome tree was performed using classify_wf workflow in GTDB-Tk (V1.7.0) based on Release 207 in Genome Taxonomy Database (https://gtdb.ecogenomic.org/) (Chaumeil et al., 2019). The trees were built using the IQ-TREE 2 program (Minh et al., 2020) with fast model selection via ModelFinder (Kalyaanamoorthy et al., 2017) and ultrafast approximation for phylogenetic bootstrap (Hoang et al., 2018) as well as approximate likelihood-ratio test for branches (Anisimova & Gascuel, 2006).

Phylogenetic trees for 16S rRNA gene sequences were identified with BLAST (Altschul et al., 1997), aligned with the SILVA alignment tool (Pruesse et al., 2007) and manually inserted in ARB database release 138.1 (Ludwig et al., 2004; Quast et al., 2013; Yarza et al., 2014). The phylogenetic tree was generated with the neighbour-joining algorithm and Jukes-Cantor distance matrix of ARB program package. The 1000 bootstrap resampling was performed to estimate the reproducibility of the partitions in the tree. Whole-genome comparison of *Halorhabdus* and *Haloferax* isolates was conducted by using three different methods: Average Nucleotide Identity (ANIb and ANIm), using JSpeciesWS web server; Average Amino acid Identity (AAI) by the AAI calculator online of Kostas lab (http://enve-omics.ce.gatech.edu/aai/index) and DDH by the Genome-to-Genome Distance Calculator 2.1 online tool (http://ggdc.dsmz.de/ggdc.php) (Richter et al., 2016; Rodriguez-R & Konstantinidis, 2014).

Transcriptomic analysis

The binary culture of *Hfx. lucertense* SVX82 + Ca. Nanohalococcus occultus SVXNc (two replicates) were grown statically in the LC medium containing xylose (200 mM) for 120 h at 40°C. Samples (5 mL) taken from cultures were used for total RNA isolation using the GeneJET RNA purification kit (Thermo Fisher Scientific) according to the manufacturer's instructions. The isolated RNAs were treated with a DNA-free™ kit (Ambion) and the amounts of RNA were determined in a NanoDrop® ND-2000 Spectrophotometer (Thermo Fisher Scientific) and by a Picogreen Qubit method (Thermo Fisher Scientific). The integrity and quality of RNA samples were evaluated by Agilent 2100 Bioanalyzer (Agilent Technologies). After rRNA depletion and DNAse treatment, the metatranscriptome analysis was done by FISABIO (Valencia, Spain) using the Illumina® NextSeq Mid Output platform with 2 × 100 bp short insert paired-end libraries (NextSeq Reagent Kit v2.5). FISABIO also performed the quality assessment and the sequence joining (forward R1 and reverse R2). Quality assessment was performed as mentioned above.

Analysis of the differential gene expression was performed using the Bioconductor R package Rsubread for Illumina read mapping against the reference genome sequence of Ca. Nanohalococcus occultus SVXNc and packages GenomicFeatures and DESeq2 for counting the mapped reads, count normalisation and fold-change estimation. The packages were run on R-4.1.3. Average $\log_2$ (fold change) values for genes composing different metabolic pathways were calculated and used for a principal component plotting using an implementation of this algorithm in PAleontological STatistics (PAST) 4.02 (http://folk.uio.no/ohammer/past/) (Hammer et al., 2001).

Proteomic analysis

Cell lysis, protein extraction and proteolytic digestion were performed as described previously (La Cono et al., 2020; Sorokin et al., 2021). Obtained peptides were further analysed by a reversed-phase liquid chromatography mass-spectrometry method (RP-LC-ESI-MS/MS) in an EASY-nLC 1000 System coupled with the Q-Exactive ultra-high field mass spectrometer (HF-MS). Peptides were loaded first onto an Acclaim PepMap 100 Trapping column (Thermo Scientific, 20 mm × 75 µm ID: 3-µm C18 resin with a 100 Å pore size) using buffer A (mobile phase A: 2% acetonitrile

[v/v], 0.1% formic acid [v/v]) and were then separated and eluted using a C18 resin analytical column Easy Spray Column (Thermo Scientific, 500 mm × 75 μm, ID: 2-μm C18 resin with a 100 Å pore size) with an integrated spray tip. A 120 min gradient of 2%–40% Buffer B (100% acetonitrile, 0.1% formic acid [v/v]) in Buffer A at a constant flow rate of 250 nL/min was used. Data acquisition was performed with a Q-Exactive HF-MS. Data were acquired using an ion spray voltage of 1.8 kV and an ion transfer temperature of 270°C. All data were acquired using data-dependent acquisition (DDA) and in positive mode with Xcalibur 4.1 software. For the MS2 scan, we selected the top 15 most-abundant precursors with charges of 2^+ to 6^+ in MS 1 scans for higher energy collisional dissociation (HCD) fragmentation with a dynamic exclusion of 27 s. The MS1 scans were acquired in the m/z range of 390–1700 Da with a mass resolution of 60,000 and automatic gain control (AGC) target of 3E6 at a maximum Ion Time (ITmax) of 20 ms. The threshold to trigger MS2 scans was 8E3; the normalised collision energy (NCE) was 27%; the resolved fragments were scanned at a mass resolution of 15,000 and AGC target value of 2E5 in an ITmax of 120 ms.

Peptide identification from raw data was carried out using MASCOT v2.4 search engine through the Protein Discoverer 2.4 Software (Thermo Scientific). Database search was performed against the SVX82 and SVXNc genome sequences. The following parameters were used for the searches: tryptic cleavage, up to two missed cleavage sites allowed, and tolerances of 10 ppm for precursor ions and 0.02 Da for MS/MS fragment ions and the searches were performed allowing optional methionine oxidation and acetylation protein N terminal, and as fixed modification, carbamidomethylation of cysteine. The false discovery rate (FDR) scores were adjusted by a percolator algorithm. The acceptance criteria for protein identifications were FDR scores <1% and at least one peptide identified with high confidence.

Etymology

Nanohalovita – Na.no.ha.lo.vi'ta. Gr. masc. n. **nanos**, a dwarf; Gr. masc. n. **hals**, salt; L. fem. n. **vita**, life; N.L. fem. n. *Nanohalovita*, dwarf salt life.

haloferacivicina – ha.lo.fe.ra.ci.vi.ci'na. N.L. neut. n. **Haloferax**, a haloarchaeal genus; L. masc. adj. **vicinus**, neighbouring; N.L. fem. adj. **haloferacivicina**, neighbouring *Haloferax*.

Nanohalococcus – Na.no.ha.lo.coc'cus. Gr. masc. n. **nanos**, a dwarf; Gr. masc. n. **hals**, salt; N.L. masc. n. **coccus** (from Gr. masc. n. **kokkos**, grain), a coccus; N.L. masc. n. *Nanohalococcus*, a dwarf salt coccus.

occultus – oc.cul'tus. L. masc. part. adj. **occultus**, hidden.

RESULTS AND DISCUSSION

Xylan-degrading enrichment and isolation of axenic and binary cultures

Using a deep-metabarcoding next-generation sequencing (NGS) platform, we previously demonstrated that nanohaloarchaea are abundant in both marine solar saltern Margherita di Savoia and Sol-Iletsk lake *Razval* reaching a maximum of about 11% and 18% of all archaeal species present, respectively (Leoni et al., 2020; Selivanova et al., 2018). Therefore, these sites were chosen for the current study. The previously designed Laguna Chitin (LC) mineral medium (La Cono et al., 2020) supplemented with birchwood xylan—as the only carbon substrate for growth and energy source—was used to select for enrich xylanolytic haloarchaea. After 2 (saltern) and 3 months (salt lakes) of static incubation at 40°C, each enrichment culture (termed BNX and SVX, respectively) was visibly turbid with a reddish hue, indicating the growth of haloarchaea. Further steps of purification, described in the *Experimental procedures*, were applied to achieve the minimal biodiversity of xylanolytic consortia (Figure S2).

The BNX and SVX enrichments were very similar in appearance. Metabarcoding analysis showed that both enrichments grown from the last dilution-to-extinction series were composed of haloarchaea belonging to the genera *Halorhabdus* and *Haloferax* as well as representatives of the phylum Ca. Nanohaloarchaeota. However, when plating a small aliquot of the final dilutions onto xylan-supplemented LC agar, only a single-colony morphotype was observed. In contrast, two types of colonies formed when xylan was replaced with D-xylose. As it was identified further by 16S rRNA gene cloning and sequencing, the xylan-utilising haloarchaea, designed as strains BNX81 and SVX81, were very similar to each other and belonged to the genus *Halorhabdus*. They were most closely related to *Halorhabdus utahensis*^{T} DSM12940 (with 99.39% of 16S rRNA gene sequence identity) and *Halorhabdus tiamatea* SARL4B (with 99.80% of 16S rRNA gene sequence identity), the two haloarchaeal species, known to possess β-xylanase and β-xylosidase (Wainø & Ingvorsen, 2003) or with predicted xylanolytic activity (Werner et al., 2014), respectively. The 16S rRNA genes of both *Haloferax* strains BNX82 and SVX82 were 100% identical to one another and to *Hfx. lucentense* strain JCM 9276, isolated from a crystalliser pond of a solar saltern near Alicante (Spain) (Gutierrez et al., 2020).

Using our previous experience in conducting host-switch experiments (La Cono et al., 2020) (Figure S2), all attempts to cultivate BNXNv and SVXNc nanohaloarchaea with either *Halorhabdus* BNX81 or SVX81 isolates on xylan have failed. On the other hand, mixing the filter-separated nanohaloarchaeal cell suspensions with corresponding *Hfx. lucentense* BNX82 and

SVX82 axenic cultures grown on D-xylose gave rise to reconstructed co-cultures. Thus, the presence of xylose-utilising *Hfx. lucentense* as a host appears to be a prerequisite for the successful cultivation of new nanohaloarchaea under given conditions, which was not the case for *Halorhabdus* isolates. In addition to the xylan-growing three-membered culture, the reconstructed xylose-utilising *Haloferax*–nanohaloarchaeon binary cultures were used to carry out studies on the microscopy, physiology and biochemistry of these organisms, as described below.

Phylogenomic identification of nanohaloarchaeal isolates

The phylogenetic positioning of novel nanohaloarchaeal strains BNXNv and SVXNc was approximated using the master alignment in SILVA Release 132SSURef NR99 (Pruesse et al., 2007) and inferred using maximum parsimony criteria within the ARB software (Ludwig et al., 2004) (Figure S3). This suggested that the closest neighbours of the BNXNv nanohaloarchaeon are the partially sequenced clones LDS1_clone18, 25, 27 and 34 (GenBank GQ374932, GQ374936, GQ374938 and GQ374944, respectively; 95.44% identity) from the Lara deep storage crystalliser pond (Australia), all belonging to Clade IV of the candidate phylum Nanohaloarchaeota (Ghai et al., 2011; Narasingarao et al., 2012). Together with uncultivated Dead Sea nanohaloarchaeal strain M3_22 (CP046106; 96.82% sequence identity) (Feng et al., 2021), the BNXNv isolate forms a distinct group in the phylum (≦92.42% sequence identities to those of other genera) and falls within the range of recently recommended values for family- and genus-level classifications (Yarza et al., 2014). It should be noted that Clade IV also contains nanohaloarchaea from the deep-sea hypersaline anoxic Lake *Hephaestus* (Mediterranean Sea), where they were found in the same abundance as haloarchaea (each group consisted of 13% of all archaeal clones) (La Cono et al., 2019). The phylogenetic positioning of the SVXNc strain revealed its deep branching position within the candidate phylum Nanohaloarchaeota, with the closest neighbouring genera not exceeding 90% of 16S rRNA gene identity: *Ca*. Nanohalobium constans 2CAF (MN178624; 90.16% sequence identity); Dead Sea nanohaloarchaea strain M3_22 (CP046106; 90.09% sequence identity) and *Ca*. Nanohalobium constans LC1Nh (CP040089; 89.97%).

The separate genus-level position of both novel nanohaloarchaeal strains was confirmed by comparative sequence analysis of a concatenated alignment of the 122 single-copy archaeal marker genes using the Genome Taxonomy Database (GTDB) framework (Parks et al., 2018) (Figure 1). Recently, it was suggested that the phylum Nanohaloarchaeota should be divided at least into three class-level groups (Rinke et al., 2021; Zhao et al., 2022). One of these proposed groups comprises the cultivated Ca. Nanohaloarchaeum antarcticus (Hamm et al., 2019), the second group consists of Ca. Nanosalinicola of uncertain taxonomic rank (that currently lacks cultivated representatives) and the third group—*Candidatus* Nanohalobia—includes cultivated strains *Ca*. Nanohalobium constans LC1Nh and 2CAF (La Cono et al., 2020; Messina et al., 2021; Oren & Garrity, 2021) and now also the BNXNv strain, which we propose to allocate in a new family, 'Ca. Nanohalovitaceae' as '*Ca*. Nanohalovita haloferacivicina' gen. nov., sp. nov. [a dwarf salt life, neighbouring *Haloferax*]. Based on our phylogenomic analyses (Figures 1 and S3), we also propose a new class 'Ca. Nanohalococcia' which includes a new order, 'Ca. Nanohalococcales' and a novel family, 'Ca. Nanohalococcaceae', accommodating the genus 'Ca. Nanohalococcus' and the species '*Ca*. Nanohalococcus occultus' SVXNc [a hidden dwarf salt coccus].

Growth physiology of three-membered and binary cultures, both containing nanohaloarchaea

Given the similarity in appearance of the xylan-degrading SVX and BNX enrichments, only the first one was used for detailed physiological and biochemical studies (the SVX enrichment). In the *Halorhabdus*—*Haloferax*—Ca. Nanohalococcus three-membered culture, xylan was completely degraded after less than 2 weeks of incubation in the LC liquid medium at 40°C. Numerous xylan oligomers were detected in the culture supernatant by high-performance anion exchange chromatography already after 24 h of cultivation and tended to shorten by the end of the first week of growth, while D-xylose was found in relatively high concentrations in culture medium supernatant only after 2 days of growth (Figure 2A). This pentose sugar most likely supported the growth of *Haloferax* SVX82, as it lacks the ability to decompose xylan (which was confirmed at the time of isolation [see above]). In turn, xylose-metabolising *Haloferax* SVX82 promotes active growth of the SVXNc nanohaloarchaeon. After 10 days of cultivation, the cell density SVXNc reached $2.1 \pm 0.4 \times 10^9$ cells/mL, slightly exceeding the density of the SVX82 host ($7.6 \pm 2.6 \times 10^8$ cells/mL) (Figure 2B). Notably, the cell density of *Halorhabdus* SVX81, the key xylan-degrading organism in the SVX consortium, did not exceed a density of $1.1 \pm 0.4 \times 10^8$ cells/mL. This suggests a superior capacity of *Haloferax* SXV82 to scavenge extracellular D-xylose, produced by SVX81 during xylan hydrolysis. The strong dominance of

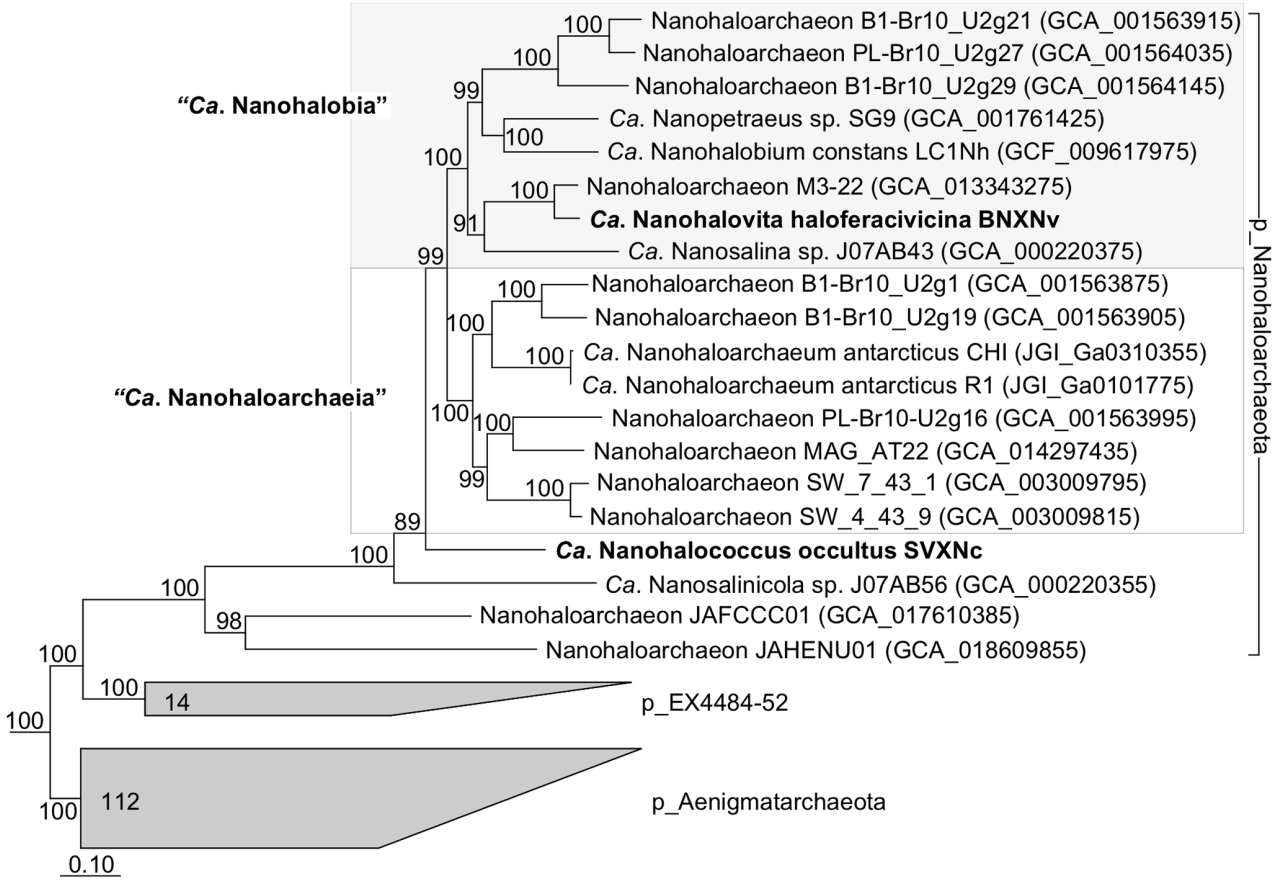

FIGURE 1 Phylogenetic placement of Ca. Nanohalococcus occultus SVXNc and Ca. Nanohalovita haloferacivicina BNXNv based on sequence analyses of a concatenated alignment of 122 single copy conserved archaeal protein markers (Parks et al., 2018) (taxonomic designations correspond to the Genome Taxonomy Data Base 207). The trees were built using the IQ-TREE 2 program with an approximate likelihood ratio test for branches. Bootstrap consensus tree is shown at the nodes. Bar, 0.10 changes per position.

SVX82 over SVX81 (39% vs. 3% of all filtered sequence reads) was also confirmed by NGS Illumina metabarcoding analysis of the xylan-degrading SVX consortium grown for 1 week (Figure S4).

To test for some influence of the ectosymbiotic nanohaloarchaeon on the host, cell densities and growth rates on D-xylose of the SVX82 axenic culture and the SVX82–SVXNc binary co-culture (both made in triplicate) were determined. As shown in Figure 2C, both the maximum specific growth rates of the host ($0.101\,h^{-1}$ [axenic culture] vs. $0.069\,h^{-1}$ [binary culture], $p = 0.002$) and the host biomass yield ($1.6 \pm 0.7 \times 10^{10}$ cells mL^{-1} [axenic culture] vs. $8.7 \pm 0.4 \times 10^{8}$ cells mL^{-1} [binary culture], $p < 0.009$) exhibited the statistically significant differences. This finding is somewhat different from what was reported in our previous study describing the chitin-degrading association of *Halomicrobium–Ca*. Nanohalobium. Although there were differences in host physiology (changes in respiratory rates and accumulation of end metabolites) cultivated in the presence or absence of the ectosymbiont, this did not affect either the maximum specific growth rate or the host biomass yield (La Cono et al., 2020).

Microscopy of nanohaloarchaeon–Haloferax associations

Field emission scanning electron microscopy (FESEM) and transmission electron microscopy (TEM) revealed that the BNXNv and SVXNc nanohaloarchaea are tiny cocci tightly attached to *Haloferax* host cells (Figures 3 and 4). It is noteworthy that while Ca. Nanohalovita BNXNv formed an association with the host cell with the median multiplicity of only one or two cells per host cell, the median multiplicity of attached Ca. Nanohalococus SVXNc was much higher: five to seven cells per host cell. This frequency of SVXNc cells attached to the single host cell is similar to that found in the *Ca*. Nanohalobium LC1Nh–*Halomicrobium* binary culture (La Cono et al., 2020; Messina et al., 2021), although the association of as many as 17 nanohaloarchaeal cells with single host cell was also quite often observed there (Figure 4G,H). FESEM and thin-section TEM imaging of the BNXNv and SVXNc co-cultures revealed contact characteristics between nanohaloarchaeal cells and the host, similar to those already observed in the *Ca*. Nanohalobium LC1Nh–*Halomicrobium* association

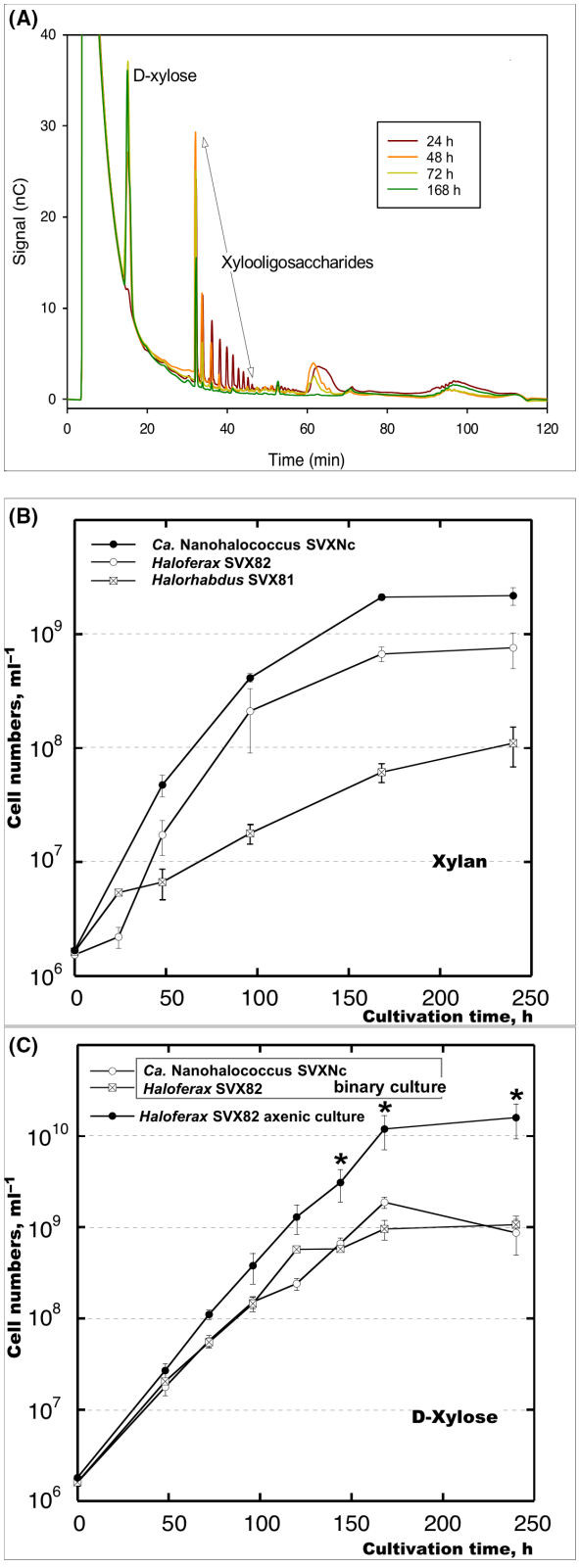

FIGURE 2 High-performance anion exchange chromatography of the supernatant of the xylan-degrading SVX three-membered culture (A) and growth of Ca. Nanohalococcus occultus SVXNc in three-membered and binary cultures on xylan (B) and xylose (C). Plotted values are means, and error bars (SDs) are based on three culture replicates. The overall significance level $p < 0.01$ is indicated by single asterisks for the host grown on xylose in axenic and binary cultures.

(La Cono et al., 2020; Messina et al., 2021). Namely, there were surface attachments with a visibly separated boundary layer that was frequently accompanied by stretching of the host envelope (Figure 3). However, no signs of nanohaloarchaeal penetration through the host cell membrane were noticed characterising the interaction as the ectosymbiontic.

Trophic relations of haloarchaea within xylan-degrading three-membered culture

Currently, there are only a few haloarchaeal species that were successfully grown on xylans, including the neutrophilic *Halorhabdus utahensis* and *Halococcides cellulosivorans* and the alkaliphilic *Natronolimnobius baerhuensis* and *Natronobiforma* cellulosivorans (Sorokin et al., 2015, 2019, 2022; Wainø & Ingvorsen, 2003). However, neither the in-depth genome analysis nor the expression of the entire genomic repertoire for complete xylan depolymerisation in these species has been assessed. Here, we present the first detailed description of genome-inferred trophic relations in a xylan-degrading three-membered culture with particular emphasis on the pivotal organisms, capable of depolymerisation of xylan, a major hemicellulose component of wood. We succeeded in the assembly and closure of the complete genomes of all members of both xylan-degrading three-membered cultures, SVX and BNX. For all six genomes, an overview of their characteristics is provided in Tables S4 and Data S1 and S2. We used these data in an attempt to understand key aspects of the trophic relations between the BNXNv and SVXNc nanohaloarchaea and their haloarchaeal host. Given the marked similarity of the *Halorhabdus* sp. SVX81 and BNX81 eco-physiological characteristics and their genomes (Table S4), we focused on only the former haloarchaeon (SVX81) for further studies.

The genome of *Halorhabdus* sp. SVX81 contains high numbers of genes encoding CAZymes, enzymes that synthesise, modify or breakdown glycosidic bonds (Henrissat & Coutinho, 2001). Among them, three acetylxylan esterases of the CE6 family of carbohydrate esterases (EC 3.1.1.72) and 48 glycosyl hydrolases (GH) belonging to 20 different families have been identified (Data S1). Such an extensive array of CAZymes points to the broad hydrolytic potential of SVX81, which likely allows this haloarchaeon to cleave, in addition to xylan, other β-glucans (cellulose and hemicelluloses such as arabinan and arabinoxylan) as well as α-glucans (such as starch and glycogen). The initial degradation of xylan appears to begin with the concerted action of six GH10 endo-β-1,4-xylanases

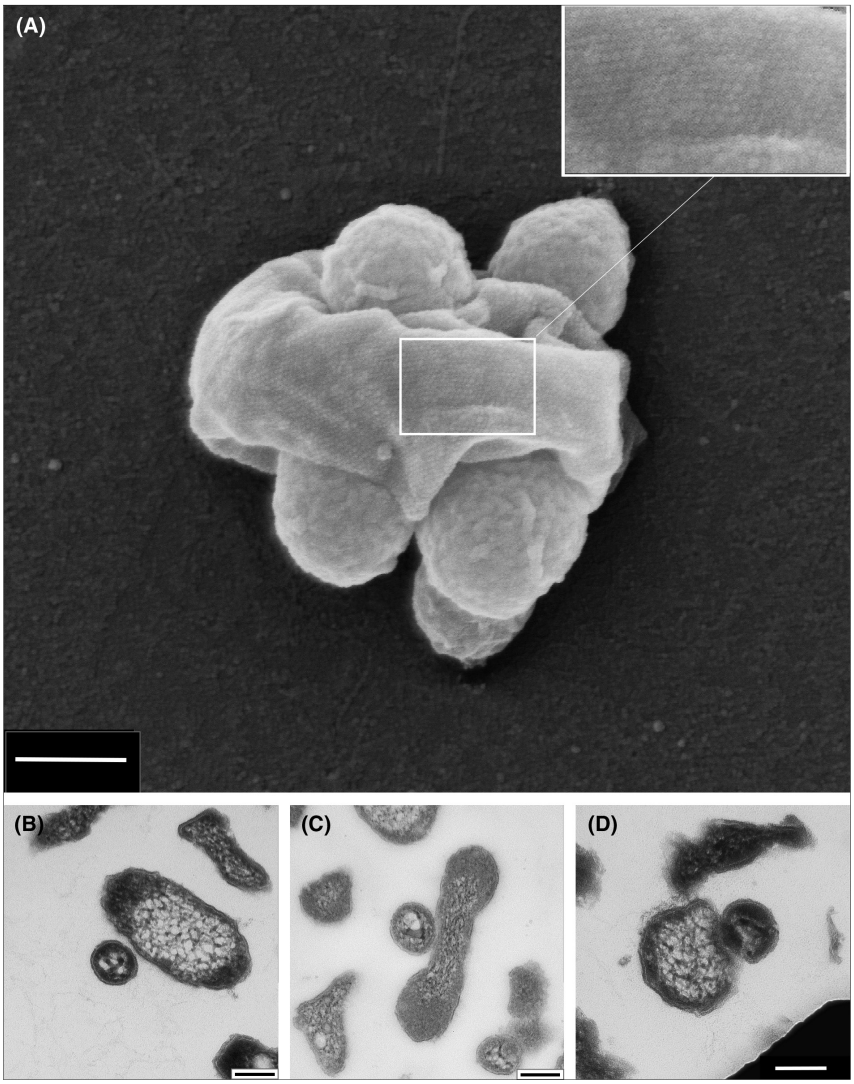

FIGURE 3 Field emission scanning (A) and transmission electron micrographs (TEM) (B–D) of Ca. Nanohalococcus occultus SVXNc and *Haloferax lucertense* SVX82 growing in the LC liquid medium supplemented with D-xylose. The images show tiny coccoidal nanohaloarchaeal cells (245 ± 35 nm in diameter) tightly adhered to the haloarchaeal host cells. The ectosymbiont causes evident invagination of the host cell surface (A, C, D). Scale bars represent 200 nm.

with different cellular localisation (both extracellular and cytoplasmic). Bioinformatic analysis revealed the presence in four GH10s of the predicted TAT/SPI signal peptides (signal peptides transported by the twin-arginine translocon *Tat* and cleaved by signal peptidase SpI). The absence of any additional transmembrane anchors strongly indicates that these endo-β-1,4-xylanases are extracellular. Notably, half of these extracellular xylanase genes (SVXHr_2167–68) are located within the so-called polysaccharide utilisation locus along with eight genes encoding endo-β-1,4-glucanases of the GH5 family (Figure S5).

As shown by high-performance anion-exchange chromatography, extracellular hydrolysis of xylan seems mediated by four aforementioned GH10 enzymes led to the formation of not only xylooligosaccharides but also D-xylose monomers (Figure 2A). The remaining cytoplasmic GH10 xylanases likely contribute to the intracellular degradation of the xylo-oligosaccharides, which enter the cell either via one of the 10 transporters of the major facilitator superfamily (MFS, SVXHr_0032, 0284, 0425, 0525, 0565, 1908, 2225–26, 2534, 2702) or via one of the two dedicated ABC-type sugar transport systems (SVXHr_0518–20; SVXHr_0591–93). Inside the cell, oligoxylans can be finally cleaved by the joint effort of three GH43 β-xylosidases (SVXHr_0230, 1878, 2135) and one exo-acting α-D-glucuronidase of the GH67 family (SVXHr_0755), to yield two monomers, D-xylose and D-glucuronic acid. It should be noted that in addition to these basic xylanases and xylosidases, SVX81 has a genomic repertoire potentially enabling complete enzymatic hydrolysis of side chains not only of beechwood xylan but also of many other side chains present in other forms of native xylans. The complex array of these side-chain hydrolytic enzymes includes acetylxylan esterases (SVXHr_1355,2169), α-D-glucuronidase (SVXHr_0755), α-L-arabinofuranosidase (SVXHr_0461), α-D-galactosidase (SVXHr_0460) and feruloyl esterases (SVXHr_1008,1616,2546) (Figure S6).

In the absence of any other annotated enzymes, D-xylose utilisation by SVX81 cells is most likely initiated by xylose isomerase (SVXHr_2114) and xylulokinase (SVXHr_0464, 2112), forming xylulose-5-phosphate. None of the other genome-sequenced archaea

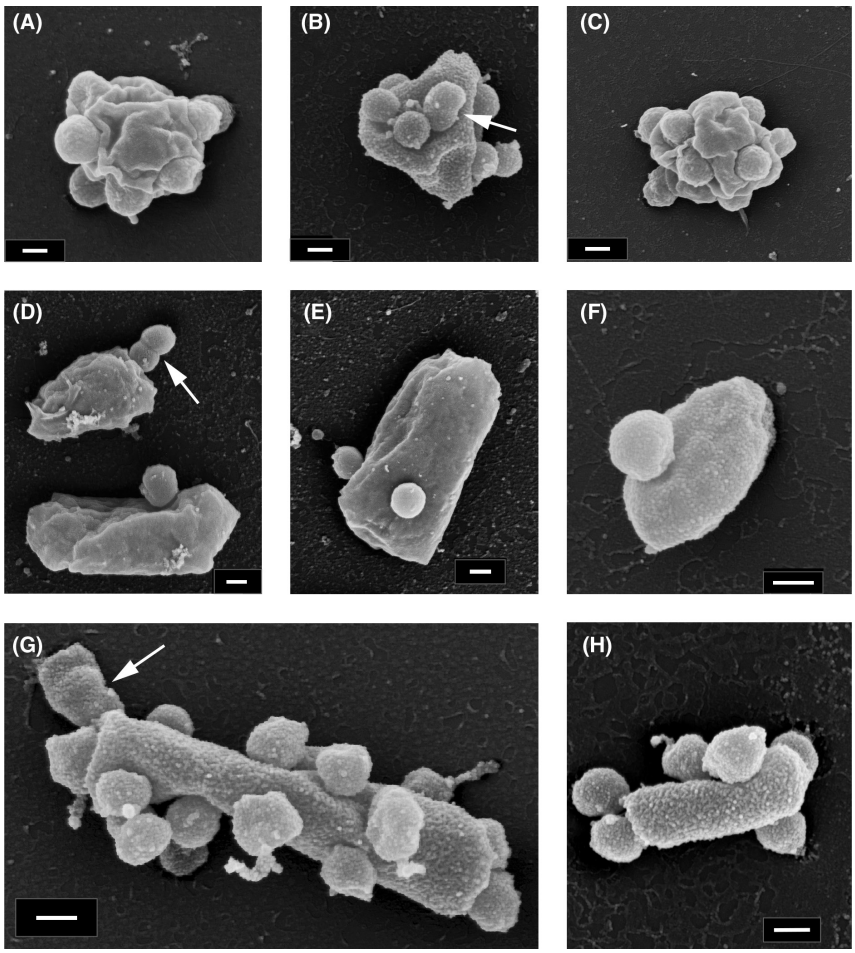

FIGURE 4 Field emission scanning electron micrographs of Ca. Nanohalococcus occultus SVXNc (A–C), Ca. Nanohalovita haloferacivicina BNXNv (D–F) and *Ca*. Nanohalobium constans LC1Nh (G, H) attached to their respective hosts, *Haloferax lucertense* BNX82 and SVX82 (A-F) and *Halomicrobium* sp. LC1Hm (G, H). The images show a strong difference in the median multiplicity of host-attached nanosymbionts: Ca. Nanohalovita BNXNv—1–2 cells/host cell; Ca. Nanohalococus SVXNc—5–7 cells/host cell; *Ca*. Nanohalobium constans LC1Nh—up to 17 cells/host cell. Dividing nanohaloarchaeal cells is indicated by white arrows. Scale bars represent 200 nm.

encodes these enzymes, with exception of three *Halorhabdus* species, *Hrb. amylolytica*, *Hrb. tiamatea* and *Hrb. utahensis*, suggesting that they may have been recently acquired from bacteria through the lateral transfer of genes (Figures S7 and S8), most likely from extremely halophilic anaerobic firmicutes of the order *Halanaerobiales* (Sutter et al., 2020). The search for a possible genetic repertoire responsible for further degradation of xylulose-5-phosphate revealed that SVX81 possesses the bacterial-type of non-oxidative phase of the pentose phosphate pathway. With regard to xylose isomerase and xylulokinase, this pathway has only recently been found in two *Halorhabdus* species (*Hrb. tiamatea* and *Hrb. utahensis*) and is missing not only in other archaea but is also missing in other *Halorhabdus* species (Sutter et al., 2020). As shown in Figure 5A, degradation of xylulose-5-phosphate in SVX81 likely involves the collective activity of D-ribulose-5-phosphate-3-epimerase, ribose-5-phosphate isomerase, transketolase and transaldolase for generation of the glycolytic intermediates, fructose-6-phosphate and glyceraldehyde-3-phosphate. With the participation of Embden–Meyerhof pathway enzymes, these intermediates can be further oxidised to pyruvate, which is ultimately used both for core metabolic processes and for providing energy via the tricarboxylic acid cycle (Sutter et al., 2020). Taken together, these data indicate that, like other *Halorhabdus* species, D-xylose in SVX81 cells appears be cleaved by the classical—non-oxidative—degradation pathway found in bacteria, but not in archaea (Sutter et al., 2020). In contrast to *Halorhabdus* species, other archaea possess the oxidative pentose phosphate pathway and degrade D-xylose to α-ketoglutarate. The combined action of the malic enzyme, phosphoenolpyruvate synthetase, and phosphoenolpyruvate carboxykinase converts this metabolite into the central phosphoenolpyruvate intermediate (Anderson et al., 2011; Sutter et al., 2020). The absence in the SVX81 genome of these enzymes, which respectively convert α-ketoglutarate via malate, oxaloacetate and pyruvatelong with the absence of fructose 1,6-bisphosphatase, indicates that *Halorhabdus* species, including *Halorhabdus* sp. SVX81, cannot use α-ketoglutarate in anabolism and therefore lack the gluconeogenesis pathway (Sutter et al., 2020).

D-glucuronic acid, the second monosaccharide released during the breakdown of beechwood xylan, is most likely converted in SVX81 cells to 2-keto-3-deoxygluconate (KDG) in a three-step pathway catalysed by the genome-collocated glucuronate isomerase, D-mannonate oxidoreductase and D-mannonate hydrolase (SVXHr_0757–59). KDG is likely

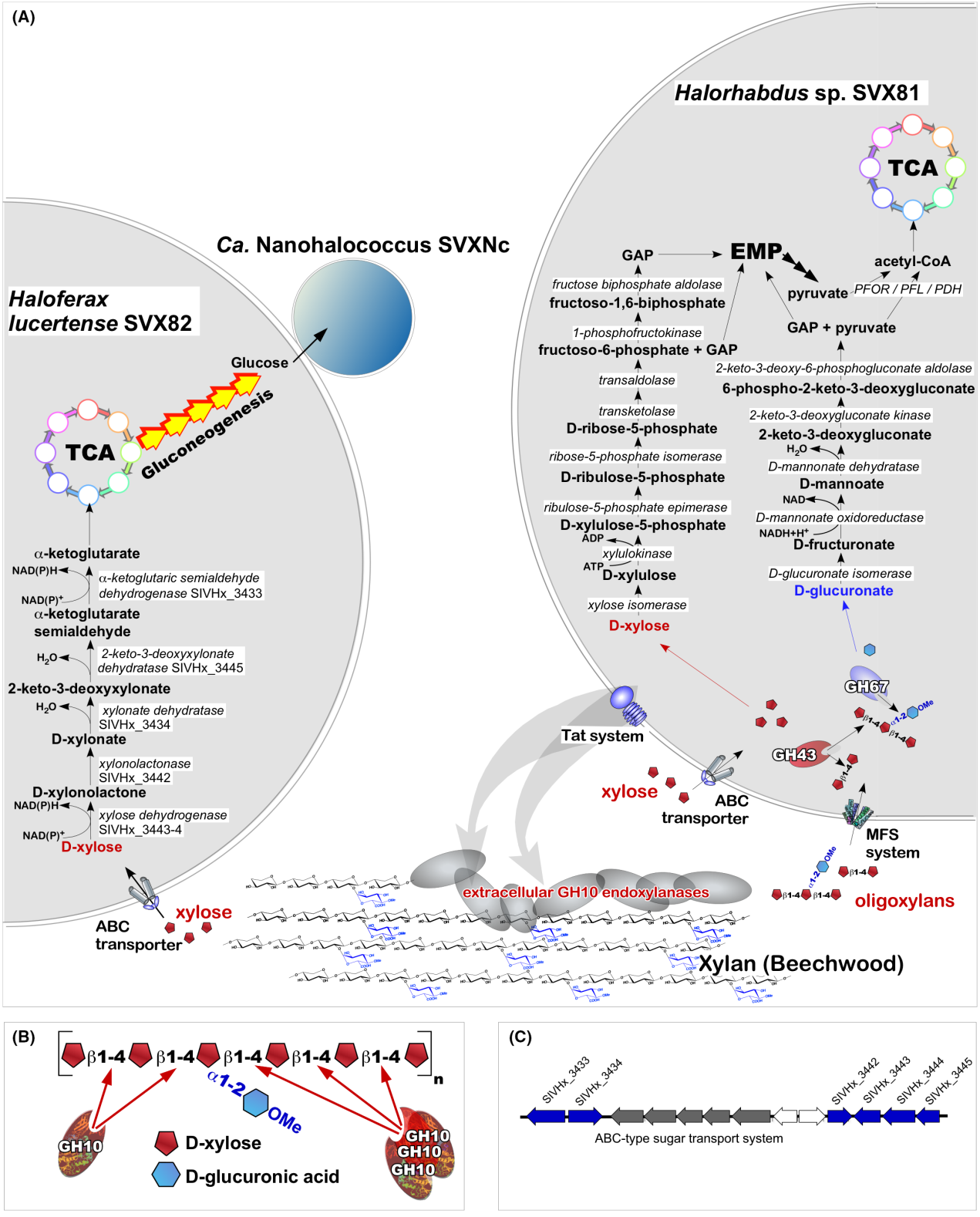

FIGURE 5 Genome-inferred trophic relations in a three-membered xylan-degrading SVX culture (A). Extracellular hydrolysis of xylan, mediated by four different endo-β-1,4-xylanases secreted by *Halorhabdus*, results in the formation of both xylooligosaccharides and D-xylose monomers (B). The non-oxidative degradation pathway of D-xylose is operative in *Halorhabdus* sp. SVX81, while *Haloferax lucertense* SVX82 uses the oxidative pathway of D-xylose degradation. All genes of this pathway form a cluster in which an ABC-type sugar transport system is also present (C). EMP, Embden-Meyerhof-Parnas pathway; GAP, glyceraldehyde-3-phosphate; MFS, transporters of the major facilitator superfamily; PDH, pyruvate dehydrogenase; PFL, pyruvate formate lyase; PFOR, pyruvate: ferredoxin oxidoreductase; TCA, tricarboxylic acid cycle.

then phosphorylated by KDG kinase (SVXHr_1094) to form 6-phospho-KGP (KDGP), which can finally be cleaved by KDGP aldolase (SVXHr_0294) to yield pyruvate and glyceraldehyde-3-phosphate, which may be involved in the Embden-Meyerhof-Parnas pathway (Figure 5A). This is only a genome-inferred speculation as the oxidative pathway of the utilisation of α-D-glucuronic acid has not been yet described in detail for haloarchaea.

The genome of the second representative of the xylan-degrading three-membered culture, *Haloferax lucertense* SVX82, contains only six genes encoding CAZymes. Among those, there are two GH3 β-glucosidases, two GH13 α-amylases and two GH15 glucoamylases (Data S3). This set of CAZymes is very poor compared to *Halorhabdus* sp. SVX81 and prevents *Hfx. lucertense* SVX82 from feeding on both xylans and oligoxylans. Thus, the extracellular formation of D-xylose monomers by the xylanolytic SVX81, confirmed by chromatography, is vital to the success of SVX82 in the xylan-degrading consortium. Genome analysis showed that in SVX82 cells, D-xylose is most likely cleaved to α-ketoglutarate via a partially promiscuous oxidative pathway (Sutter et al., 2017), which involves specific D-xylose dehydrogenases, xylonolactonase and xylonate dehydratase (Figure 5A). Following this, α-ketoglutarate is formed by 2-keto-3-deoxyxylonate dehydratase and α-ketoglutarate semialdehyde dehydrogenase. The genes for this pathway form a cluster in which an ABC-type sugar transport system (SVXHx_3436–40) has been identified, suggesting that D-xylose is the most likely natural substrate for this transport system (Figure 5C). Unlike the xylanolytic SVX81, SVX82 possesses all the enzymes of gluconeogenesis, as well as the malic enzyme (SVXHx_2168, 2411) and phosphoenolpyruvate synthetase (SVXHx_0770), which catalyse the conversion of α-ketoglutarate to phosphoenolpyruvate.

Benefits of haloarchaeal xylan degradation for nanohaloarchaea

For both the *Nanohaloccocus* and *Nanohalovita* genomes, an overview of their characteristics is presented in Data S1–S3 and Tables S1 and S2. Like other members of the monophyletic superphylum DPANN (this acronym is derived from Diapherotrites, Parvarchaeota, Aenigmarchaeota, Nanoarchaeota and Nanohaloarchaea candidate phyla) described so far, the newly cultivated nanohaloarchaea BNXNv and SVXNc have very reduced genomes (1,046,959 bp and 948,351 bp, respectively) with only a rudimentary anabolic capability and an almost complete absence of enzymes required for the biosynthesis of nucleotides, amino acids, lipids, vitamins, and cofactors. Thus, association with the host is absolutely essential for their growth and ecological prosperity. Based on the cultivation and genome data, the BNXNv and SVXNc nanohaloarchaea, like *Ca.* Nanohalobium LC1Nh are obligate anaerobic and aerotolerant fermenters, devoid of any respiratory complexes, except for the ATPase complex V, with a complete set of enzymes involved in the processes of glycolysis/gluconeogenesis and glycogen turnover.

As regards the fermentation of sugars, the genomes of Ca. Nanohaloccocus and Ca. Nanohalovita do not contain any of the enzymes implicated in D-xylose or D-glucuronic acid metabolism. Thus, in order to survive in the xylanolytic BNX and SVX consortia, they likely must uptake the host-synthesised (mono)saccharides that they are able to metabolise. Research on the metabolic capacities and nutritional requirements of nanohaloarchaea, as well as other DPANN archaea, is still in its infancy. Based on genome analyses, however, it has been suggested that *N*-acetyl-glucosamine (GlcNAc) and glucose are among the principal monosaccharides taken up and utilised by nanohaloarchaeal ectosymbionts (La Cono et al., 2020).

Here, we hypothesised that the presence of gluconeogenesis in the *Haloferax* versus the gluconeogenesis-deficient xylanolytic *Halorhabdus*, may be very important among other factors by which the sugar-fermenting nanohaloarchaeal symbiont selects the host. Some evidence that consistent with this hypothesis is presented below. We did not expect that the *Haloferax* host would be able to synthesise GlcNAc in quantities sufficient to support the growth of the ectosymbiont, so we analysed the intracellular concentration of glucose-6-phosphate, one of the final metabolites of the gluconeogenesis. An axenic host culture of *Haloferax* SVX82 was used by way of comparison. Given the substantial inhibition of host growth in binary culture versus symbiont-free culture that was noted above, some differences in the intracellular concentration of glucose-6-phosphate were expected, but not as great as those that were measured (Table S5). The amount of this gluconeogenic metabolite in the axenic culture of *Haloferax* SVX82 did not exceed 0.40 ± 0.08 mM, which corresponds well with the known intracellular glucose-6-phosphate levels reported for other gluconeogenic microorganisms (0.3–1.0 mM) (Aiello et al., 2002). In contrast, these concentrations were measured during the current study in the *Haloferax* – Ca. Nanohalococcus binary culture reached values of 19.15 ± 0.57 mM, i.e., almost 50 times higher (Table S5). We were aware that the presence of gluconeogenic nanohaloarchaea in the binary culture could influence the final calculation of the total intracellular concentration of glucose-6-phosphate, so we calculated their approximate total cell volume in the binary culture

(see Experimental procedures). Even considering that Ca. Nanohalococcus SVXNc formed an association with the host cell at a median multiplicity of six cells per host cell (with all host cells associated with nanohaloarchaea), the total biomass (as biovolume) of nanohaloarchaea did not exceed 2% of the total (*Haloferax* + nanohaloarchaea) biomass. In addition, the expression of gluconeogenic enzyme fructose 1,6-bisphosphatase Fbp (SVXNc_0148) was checked in the Ca. Nanohalococcus's transcriptome (Data S1). Normalised values of 163 ± 9 fragments per kilobase of gene per million mapped fragments (FPKM) indicated that this enzyme was expressed, although at significantly lower levels than the glycolytic enzyme, phosphofructokinase Pfk2 (SVXNc_0128) (380 ± 43 FPKM). The predominance of glycolysis over gluconeogenesis in Ca. Nanohalococcus cells was further confirmed by proteome analysis (Data S3). The normalised spectral abundance factor (NSAF), calculated for phosphofructokinase Pfk2 (SVXNc_0128), was about 0.138 ± 0.037, while for fructose 1,6-bisphosphatase Fbp (SVXNc_0148), this value could not be determined due to the presence of Fbp-related unique peptides in only one of three analysed replicas (Data S3).

Taken together, these data suggest that the increase in the number of end products of gluconeogenesis in *Haloferax* host cells indeed can correspond to the demand for carbon and energy source in the ectosymbiont Ca. Nanohalococcus. Although this has yet to be experimentally validated, the direct uptake of glucose-6-phosphate from the host, rather than the uptake of glucose synthesised de novo, is more energetically beneficial for the ectosymbiont since such a metabolite can directly enter into catabolic processes without consuming a single ATP molecule necessary for its formation from glucose. Other aspects of the trophic interaction between ectosymbiont and host, especially those that cause drastic changes in the host growth rates and biomass yield (Figure 2C), also require a more detailed study in the future.

So far, we did not find evidence of any mutualistic relationship between *Haloferax* and Ca. Nanohalococcus, as previously described for another haloarchaea–nanohaloarchaea co-cultures (La Cono et al., 2020). As noted above, *Haloferax* possesses all glycosyl hydrolases, that are required to degrade α-glucans and can actively grow in axenic culture on both starch and glycogen (data not shown). While the symbiont might be beneficial to the host under some, as yet unknown, conditions, in the given xylan-decomposing association, Ca. Nanohalococcus seems to function purely as an ectoparasite. In this association, in addition to all other necessary metabolites, the nanohaloarchaeon likely uptakes end products of gluconeogenesis from *Haloferax lucertense*, which in turn acts as a scavenger of xylan-degradation products produced by a primary xylan hydrolytic *Halorhabdus* species (Figure 5).

CONCLUSIONS, IMPLICATIONS AND UNRESOLVED QUESTIONS

This study has doubled the number of cultivated genera representing the phylum Ca. Nanohaloarchaeota, an extremely halophilic archaeal lineage within the DPANN superphylum, and has demonstrated that they are an active ecophysiological component of polysaccharide-degrading microbial communities in hypersaline environments. The host–symbiont systems described herein did not reveal any mutual interdependence, as previously demonstrated for *Ca*. Nanohalobium and its chitinolytic *Halomicrobium* host (La Cono et al., 2020). Nevertheless, we have documented important changes in the metabolic activity of the *Haloferax* host in response to the presence of the symbiont. Their associations are part of a complex and diverse range of interactions that enable the growth of the diminutive nanohaloarchaea with a reduced genome. While some nanohaloarchaea are symbionts that enable their hosts to grow on different polysaccharides, others employ an essentially parasitic relationship with their hosts and rely entirely on them. Consequently, the nanohaloarchaea–host interactions are generally less clear-cut and more nuanced.

Potential implications and questions in relation to biotechnology and sustainability development goals

The effective breakdown of necromass and organic substances by the saprotrophic microorganisms that can drive the cycling of nutrients is imperative to SDG 6 'Clean water and sanitation'. Conversely, halotolerant/halophilic saprotrophs are sometimes implicated in the rotting of wooden structures constructed in seawater, other saline waters and brines including houses and other buildings, boats/ships, house-boats/pontoons, jetties/docks/harbours and bridges so wood is often treated with antimicrobial preservatives or paints that are toxic so can contaminate food chains and endanger the environment, wildlife, and human health (Blanchette, 2010; Jorens & Schepens, 1993), an issue pertinent to SDGs 3 'Good health and well-being', 11 'Sustainable cities and communities' and 14 'Life below water'. Wood-degrading microbes, including halophiles, can play roles in the production of biofuels (Amoozegar et al., 2019), an issue relevant to SDGs 8 'Decent work and economic growth', 9 'Industry, innovation and infrastructure', 12 'Responsible consumption and production' and 13 'Climate action'. Global climate change, agricultural irrigation and human overpopulation are causing desertification and salinisation

of soils and water bodies and are increasing the salinity of the Dead Sea (location), Great Salt Lake (Utah, USA) and other large-scale bodies of saline water or brine (Baxter & Butler, 2020; Saccò et al., 2021; Wurtsbaugh et al., 2017). This has implications for the cycling of nutrients by halotolerant/halophilic microbes and relates to SDGs 13 'Climate action', 14 'Life below water' and 15 'Life on land' (Anand et al., 2023; Cavicchioli et al., 2019).

It may seem counter-intuitive that xylan degradation, that releases carbon into the atmosphere as CO_2, might be considered in any way consistent with SDGs. However, if wood and other plant biomass were not degraded then this would impair ecosystem function in many environments where saprotrophs would not be disadvantaged (thus impacting grazers, predators and symbionts of saprotrophs), and many environments would become chocked with dead plant material. Furthermore, fresh plant biomass captures carbon so is effectively neutral in terms of contributing CO_2 (unless gas, oil, peat and coal the burning of which releases carbon into the atmosphere that would otherwise remain stored from thousands or millions of years ago).

The ecophysiological nuances of saprotrophic activity in salt-containing waters (including the breakdown of wood) are pertinent to those SDGs for which degradation is desirable as well as those where it is not. In this context, there are still outstanding questions about the degradation of xylan: how much dead plant material is situated in/ subjected to high-salt conditions; do nanohaloarchaea ever play roles in the purification of brine waters and/or rotting wooden structures; how can theory-based approaches be utilised to model the implications of climate change on nutrient cycling by halophiles (Hallsworth et al., 2023); can nanohaloarchaea (given their intimate dependence on other organisms) act as indicators of pollution by pesticides, wood preservatives or other substances or even as environmental indicators that are pertinent the health of eukaryotes including humans and what—if any—is the commercial potential of nanohaloarchaea or extreme halophilic polysaccharide-degrading consortia which they reside? Indeed, the biotechnological value of polysaccharide-degrading halophiles/halophilic communities (including those that degrade xylan) may include:

- screening of polysaccharide-degrading halophiles for potentially useful enzymes that can be utilised as stable and functional biocatalysts both in solvent-based and ionic liquid systems (Dumorné et al., 2017; Kasirajan & Maupin-Furlow, 2021; Mesbah & Wiegel, 2017);
- halotolerant and halo(alkalo)philic microbes (including xylan-degraders) can also be a good source of enzymes that are stable at high temperatures or high pH (Wainø & Ingvorsen, 2003; Liao et al., 2018; Sun et al., 2021);
- xylan-degrading halophiles have the potential for biofuel production (Amoozegar et al., 2019; Kasirajan & Maupin-Furlow, 2021), and their xylanases also have applications in pulp and paper production, bioleaching and production of detergents (Javid & Zarei, 2021) or compositing and bioconversion of seaweed wastes (Parab et al., 2017);
- it is plausible that polysaccharide-degrading halophiles or their enzymes have value as feed additives to promote digestion in ruminants that live in arid regions (Ghadikolaei et al., 2019);
- and to use as soil inocula to help to bring soils into cultivation that are currently marginal due to aridification/salinisation (Timmis & Ramos, 2021).

AUTHOR CONTRIBUTIONS

Violetta La Cono: Conceptualization (equal); data curation (equal); funding acquisition (equal); investigation (equal); methodology (equal). **Enzo Messina:** Data curation (equal); formal analysis (equal); resources (equal); software (equal). **Oleg Reva:** Data curation (equal); formal analysis (equal); software (equal); validation (equal). **Francesco Smedile:** Data curation (equal); formal analysis (equal); software (equal); validation (equal). **Gina La Spada:** Data curation (equal); formal analysis (equal); methodology (equal); software (equal). **Francesca Crisafi:** Data curation (equal); formal analysis (equal); methodology (equal). **Laura Marturano:** Formal analysis (equal); methodology (equal). **Elena A. Selivanova:** Data curation (equal); methodology (equal); resources (equal). **Olga V. Golyshina:** Supervision (equal); validation (equal); writing – review and editing (equal). **Peter Golyshin:** Validation (equal); writing – review and editing (equal). **Manfred Rohde:** Data curation (equal); formal analysis (equal); methodology (equal). **Mart Krupovic:** Formal analysis (equal); software (equal); writing – original draft (equal). **Alexandr Y. Merkel:** Methodology (equal); software (equal). **Dmitry Y. Sorokin:** Conceptualization (equal); formal analysis (equal); validation (equal); writing – review and editing (equal). **Michail M Yakimov:** Conceptualization (equal); data curation (equal); investigation (equal); supervision (equal); validation (equal); writing – original draft (equal); writing – review and editing (equal).

ACKNOWLEDGEMENTS

We thank Luigi R. Ceci (Institute of Biomembranes, Bioenergetics and Molecular Biotechnologies, IBIOM-CNR, Bari, Italy) for kind permission and assistance with sampling in the crystalliser pond *Cappella* of solar salterns of Bari and Aharon Oren (The Hebrew University of Jerusalem, Israel) for correcting the etymology of the proposed names for the new nanohaloarchaea. JEH wishes to thank Guilherme T.P. Brancini (Universidade de São Paulo, Brazil), Ram Karan (King Abdullah University of Science and Technology—KAUST—Saudi Arabia),

Rekha S. Singhal (Institute of Chemical Technology—Mumbai, India), and Kenneth Timmis (Institute of Microbiology, Technical University Braunschweig, Germany) for useful discussion. This study was partially supported by grants from the INMARE Project (Contract 2634486) and FUTURENZYMES Project (Contract 101000327), both funded by the European Union's Horizon 2020 Research Program. OVG and PNG acknowledge support from the Centre for Environmental Biotechnology Project, partly funded by the European Regional Development Fund via the Welsh Assembly Government. DYS was supported by the SYAM-Gravitation Program of the Dutch Ministry of Education, Culture and Science (grant 24002002). MK was supported by Agence Nationale de la Recherche (grant ANR-20-CE20-0009). MF also acknowledges financial support under grants PID2020-112758RB-I00, PDC2021-121534-I00 and TED2021-130544B-I00 from the Ministerio de Ciencia e Innovación, Agencia Estatal de Investigación (AEI) (Digital Object Identifier 10.13039/501100011033) and the European Union ('NextGeneration EU/PRTR'). The authors acknowledge the unit CAI Técnicas Biológicas (Unidad de Proteómica) for supporting the proteomic analysis and Francisco J. Plou (ICP, CSIC) for giving access to HPLC resources.

CONFLICT OF INTEREST STATEMENT

The authors declare that they have no current or potential competing financial interests.

DATA AVAILABILITY STATEMENT

All statements regarding data availability, finding resources and conflict of interest disclosure have been provided.

DATA DEPOSITION

All (meta)genomic and transcriptomic information is available under GenBank BioProject ID PRJNA865582; BioSamples SAMN30630960, SAMN30630938, SAMN30630946, SAMN30631035, SAMN30630966, SAMN30631033, SAMN30120999, SAMN30121000, SAMN30121001, SAMN30121002, SAMN30121003 and SAMN30121004; genome accession no. CP104322 for *Halorhabdus* sp. SVX81, genome accession no. CP104395 for Ca. Nanohalococcus occultus SVXNc, genome accession nos. CP104741 (chromosome), CP104742 (plasmid 1), CP104743 (plasmid 2) and CP104744 (plasmid 3) for *Haloferax lucertense* SVX82; genome accession no. CP107254 for *Halorhabdus* sp. BNX81, genome accession no. CP107255 for Ca. Nanohalovita haloferacivicina BNXNv, genome accession nos. CP106966 (chromosome), CP106967 (plasmid 1), CP106968 (plasmid 2), CP106969 (plasmid 3) and CP106970 (plasmid 4) for *Haloferax lucertense* BNX82. Transcriptomic raw data are available under accession SRR21676140-SRR216761401. The mass spectrometry proteomics data have been deposited in the ProteomeXchange Consortium via the PRIDE partner repository with the data set identifier PXD036877.

ORCID

Violetta La Cono https://orcid.org/0000-0002-3306-4938
Enzo Messina https://orcid.org/0000-0001-9042-0014
Oleg Reva https://orcid.org/0000-0002-5459-2772
Francesco Smedile https://orcid.org/0000-0001-8882-284X
Gina La Spada https://orcid.org/0000-0003-4768-182X
Francesca Crisafi https://orcid.org/0000-0002-4917-893X
Manuel Ferrer https://orcid.org/0000-0003-4962-4714
Elena A. Selivanova https://orcid.org/0000-0002-5155-1801
Olga V. Golyshina https://orcid.org/0000-0001-5132-6850
Peter N. Golyshin https://orcid.org/0000-0002-5433-0350
Manfred Rohde https://orcid.org/0000-0003-0522-3580
Mart Krupovic https://orcid.org/0000-0001-5486-0098
Alexander Y. Merkel https://orcid.org/0000-0002-6089-9500
Dimitry Y. Sorokin https://orcid.org/0000-0001-9900-4412
John E. Hallsworth https://orcid.org/0000-0001-6797-9362
Michail M. Yakimov https://orcid.org/0000-0003-1418-363X

REFERENCES

Aiello, D.P., Fu, L., Miseta, A. & Bedwell, D.M. (2002) Intracellular glucose 1-phosphate and glucose 6-phosphate levels modulate Ca^{2+} homeostasis in *Saccharomyces cerevisiae*. *The Journal of Biological Chemistry*, 277, 45751–45758.

Altschul, S.F., Madden, T.L., Schäffer, A.A., Zhang, J., Zhang, Z., Miller, W. et al. (1997) Gapped BLAST and PSI-BLAST: a new generation of protein database search programs. *Nucleic Acids Research*, 25, 3389–3402.

Amoozegar, M.A., Safarpour, A., Noghabi, K.A., Bakhtiary, T. & Ventosa, A. (2019) Halophiles and their vast potential in biofuel production. *Frontiers in Microbiology*, 10, 1895.

Anand, S., Hallsworth, J.E., Timmis, J., Verstraete, W., Casadevall, A., Ramos, J.L. et al. (2023) Weaponising microbes for peace. *Microbial Biotechnology*, 16, in press. Available from: https://doi.org/10.1111/1751-7915.14224

Anderson, I., Scheuner, C., Göker, M., Mavromatis, K., Hooper, S.D., Porat, I. et al. (2011) Novel insights into the diversity of catabolic metabolism from ten haloarchaeal genomes. *PLoS One*, 6, e20237.

Andrei, A.Ş., Banciu, H.L. & Oren, A. (2012) Living with salt: metabolic and phylogenetic diversity of archaea inhabiting saline ecosystems. *FEMS Microbiology Letters*, 330, 1–9.

Anisimova, M. & Gascuel, O. (2006) Approximate likelihood-ratio test for branches: a fast, accurate, and powerful alternative. *Systematic Biology*, 55, 539–552.

Baxter, B.K. & Butler, J.K. (Eds.). (2020) *Great salt Lake biology: a terminal lake in a time of change*. Cham: Springer.

Belilla, J., Moreira, D., Jardillier, L., Reboul, G., Benzerara, K., López-García, J. et al. (2019) Hyperdiverse archaea near

life limits at the polyextreme geothermal Dallol area. *Nature Ecology & Evolution*, 3, 1552–1561.
Benison, K.C., O'Neill, W.K., Blain, D. & Hallsworth, J.E. (2021) Water activities of acid brine lakes approach the limit for life. *Astrobiology*, 21, 729–740.
Blanchette, R.A. (2010) Microbial degradation of wood from aquatic and terrestrial environments. In: Mitchell, R. & McNamara, C.J. (Eds.) *Cultural heritage microbiology: fundamental studies in conservation science*. Washington, DC: ASM Press, pp. 179–218.
Boetius, A. & Joye, S. (2009) Thriving in salt. *Science*, 324, 1523–1525.
Cavalazzi, B., Barbieri, R., Gómez, F., Capaccioni, B., Olsson-Francis, K., Pondrelli, M. et al. (2019) The Dallol geothermal area, northern Afar (Ethiopia)—an exceptional planetary field analog on earth. *Astrobiology*, 19, 553–578.
Cavicchioli, R., Ripple, W.J., Timmis, K.N., Azam, F., Bakken, L.R., Baylis, M. et al. (2019) Scientists' warning to humanity: microorganisms and climate change. *Nature Reviews Microbiology*, 17, 569–586.
Chaumeil, P.A., Mussig, A.J., Hugenholtz, P. & Parks, D.H. (2019) GTDB-Tk: a toolkit to classify genomes with the genome taxonomy database. *Bioinformatics*, 36, 1925–1927.
Conway, E.J. & Downey, M. (1950) An outer metabolic region of the yeast cell. *The Biochemical Journal*, 47, 347–355.
Crits-Christoph, A., Gelsinger, D.R., Ma, B., Wierzchos, J., Ravel, J., Davila, A. et al. (2016) Functional interactions of archaea, bacteria and viruses in a hypersaline endolithic community. *Environmental Microbiology*, 18, 2064–2077.
Di Meglio, L., Santos, F., Gomariz, M., Almansa, C., López, C., Antón, J. et al. (2016) Seasonal dynamics of extremely halophilic microbial communities in three Argentinian salterns. *FEMS Microbiology Ecology*, 92, fiw184.
Drever, J.I. (1988) *The geochemistry of natural waters*. Englewood Cliffs: Prentice hall, New Jersey, p. 437.
Dumorné, K., Córdova, D.C., Astorga-Eló, M. & Renganathan, P. (2017) Extremozymes: a potential source for industrial applications. *Journal of Microbiology and Biotechnology*, 27, 649–659.
Feng, Y., Neri, U., Gosselin, S., Louyakis, A.S., Papke, R.T., Gophna, U. et al. (2021) The evolutionary origins of extreme halophilic archaeal lineages. *Genome Biology and Evolution*, 13, evab166.
Ghadikolaei, K.K., Sangachini, E.D., Vahdatirad, V., Noghabi, K.A. & Zahiri, H.S. (2019) An extreme halophilic xylanase from camel rumen metagenome with elevated catalytic activity in high salt concentrations. *AMB Express*, 9, 86.
Ghai, R., Pašić, L., Fernández, A.B., Martin-Cuadrado, A.B., Mizuno, C.M., McMahon, K.D. et al. (2011) New abundant microbial groups in aquatic hypersaline environments. *Scientific Reports*, 1, 135.
Gomariz, M., Martínez-García, M., Santos, F., Rodriguez, F., Capella-Gutiérrez, S., Gabaldón, T. et al. (2015) From community approaches to single-cell genomics: the discovery of ubiquitous hyperhalophilic *Bacteroidetes* generalists. *The ISME Journal*, 9, 16–31.
Grant, S., Grant, W.D., Jones, B.E., Kato, C. & Li, L. (1999) Novel archaeal phylotypes from an east African alkaline saltern. *Extremophiles*, 3, 139–145.
Gutierrez, G.M., Kamekura, M., Holmes, M.L., Dyall-Smith, M.L. & Ventosa, A. (2020) Taxonomic characterization of *Haloferax* sp. ("H. alicantei") strain aa 2.2: description of *Haloferax lucentensis* sp. nov. *Extremophiles*, 6, 479–483.
Hallsworth, J.E. (2019) Microbial unknowns at the saline limits for life. *Nature Ecology and Evolution*, 3, 1503–1504.
Hallsworth, J.E., Udaondo, Z., Pedrós-Alió, C., Höfer, J., Benison, K.C., Lloyd, K.G. et al. (2023) Scientific novelty beyond the experiment. *Microbial Biotechnology*, 16, Available from: https://doi.org/10.1111/1751-7915.14222
Hallsworth, J.E., Yakimov, M.M., Golyshin, P.N., Gillion, J.L.M., D'Auria, G., Alves, F.L. et al. (2007) Limits of life in $MgCl_2$-containing environments: chaotropicity defines the window. *Environmental Microbiology*, 9, 803–813.
Hamm, J.N., Erdmann, S., Eloe-Fadrosh, E.A., Angeloni, A., Zhong, L., Brownlee, C. et al. (2019) Unexpected host dependency of Antarctic Nanohaloarchaeota. *Proceedings of the National Academy of Sciences of the United States of America*, 116, 14661–14670.
Hammer, Ø., Harper, D.A. & Ryan, P.D. (2001) PAST: paleontological statistics software package for education and data analysis. *Palaeontologia Electronica*, 4, 9.
Henrissat, B. & Coutinho, P.M. (2001) Classification of glycoside hydrolases and glycosyltransferases from hyperthermophiles. *Methods in Enzymology*, 330, 183–201.
Hoang, D.T., Chernomor, O., Von Haeseler, A., Minh, B.Q. & Vinh, L.S. (2018) UFBoot2: improving the ultrafast bootstrap approximation. *Molecular Biology and Evolution*, 35, 518–522.
Javid, H. & Zarei, A. (2021) Short note on biotechnological application of halophilic enzymes. *Journal of Microbiology and Biotechnology*, 6, 000200.
Jorens, P.G. & Schepens, P.J. (1993) Human pentachlorophenol poisoning. *Human & Experimental Toxicology*, 12, 479–495.
Kalyaanamoorthy, S., Minh, B.Q., Wong, T.K., Von Haeseler, A. & Jermiin, L.S. (2017) ModelFinder: fast model selection for accurate phylogenetic estimates. *Nature Methods*, 14, 587–589.
Karray, F., Ben Abdallah, M., Kallel, N., Hamza, M., Fakhfakh, M. & Sayadi, S. (2018) Extracellular hydrolytic enzymes produced by halophilic bacteria and archaea isolated from hypersaline lake. *Molecular Biology Reports*, 45, 1297–1309.
Kasirajan, L. & Maupin-Furlow, J.A. (2021) Halophilic archaea and their potential to generate renewable fuels and chemicals. *Biotechnology and Bioengineering*, 118, 1066–1090.
La Cono, V., Bortoluzzi, G., Messina, E., La Spada, G., Smedile, F., Giuliano, L. et al. (2019) The discovery of Lake Hephaestus, the youngest athalassohaline deep-sea formation on Earth. *Scientific Reports*, 9, 1679.
La Cono, V., Messina, E., Rohde, M., Arcadi, E., Ciordia, S., Crisafi, F. et al. (2020) Symbiosis between nanohaloarchaeon and haloarchaeon is based on utilization of different polysaccharides. *Proceedings of the National Academy of Sciences of the United States of America*, 117, 20223–20234.
Lange, C., Zerulla, K., Breuert, S. & Soppa, J. (2011) Gene conversion results in the equalization of genome copies in the polyploid haloarchaeon *Haloferax volcanii*. *Molecular Microbiology*, 80, 666–677.
Lee, C.J.D., McMullan, P.E., O'Kane, C.J., Stevenson, A., Santos, I.C., Roy, C. et al. (2018) NaCl-saturated brines are thermodynamically moderate, rather than extreme, microbial habitats. *FEMS Microbiology Reviews*, 42, 672–693.
Leoni, C., Volpicella, M., Fosso, B., Manzari, C., Piancone, E., Dileo, M.C.G. et al. (2020) A differential metabarcoding approach to describe taxonomy profiles of *Bacteria* and *Archaea* in the saltern of Margherita di Savoia (Italy). *Microorganisms*, 8, 936.
Li, J., Gao, Y., Dong, H. & Sheng, G.P. (2022) Haloarchaea, excellent candidates for removing pollutants from hypersaline wastewater. *Trends in Biotechnology*, 40, 226–239.
Liao, Z., Holtzapple, M., Yan, Y., Wang, H., Li, J. & Zhao, B. (2018) Insights into xylan degradation and haloalkaline adaptation through whole-genome analysis of *Alkalitalea saponilacus*, an anaerobic haloalkaliphilic bacterium capable of secreting novel halostable xylanase. *Genes*, 10, 1.
Ludwig, W., Strunk, O., Westram, R., Richter, L., Meier, H., Yadhukumar et al. (2004) ARB: a software environment for sequence data. *Nucleic Acids Research*, 32, 1363–1371.
Magoč, T. & Salzberg, S.L. (2011) FLASH: fast length adjustment of short reads to improve genome assemblies. *Bioinformatics*, 27, 2957–2963.

Malik, A.D. & Furtado, I.J. (2019) Cellulase-free xylanase by *Halococcus thailandensis* GUMFAS7 and *Halorubrum saccharovorum* GUMFAS1—bionts of a sponge *Cinachyrella cavernosa*. *Microbiology*, 88, 212–219.

Martínez, J.M., Escudero, C., Rodríguez, N., Rubin, S. & Amils, R. (2021) Subsurface and surface halophile communities of the chaotropic Salar de Uyuni. *Environmental Microbiology*, 23, 3987–4001.

Mesbah, N.M. & Wiegel, J. (2017) A halophilic, alkalithermostable, ionic liquid-tolerant cellulase and its application in in situ saccharification of rice straw. *Bioenergy Research*, 10, 583–591.

Messina, E., La Cono, V., Rhode, M., Sorokin, D. Y., Oren, A., and Yakimov, M. M. (2021) *Candidatus Nanohalobium*. In *Bergey's manual of systematics of archaea and bacteria*, Online edn. Reysenbach, A.-L. (ed). Hoboken, NJ: John Wiley & Sons Inc, pp. 1–5.

Minh, B.Q., Schmidt, H.A., Chernomor, O., Schrempf, D., Woodhams, M.D., von Haeseler, A. et al. (2020) IQ-TREE 2: new models and efficient methods for phylogenetic inference in the genomic era. *Molecular Biology and Evolution*, 37, 1530–1534.

Mora-Ruiz, M.D.R., Cifuentes, A., Font-Verdera, F., Pérez-Fernández, C., Farias, M.E., González, B. et al. (2018) Biogeographical patterns of bacterial and archaeal communities from distant hypersaline environments. *Systematic and Applied Microbiology*, 41, 139–150.

Narasingarao, P., Podell, S., Ugalde, J.A., Brochier-Armanet, C., Emerson, J.B., Brocks, J.J. et al. (2012) De novo metagenomic assembly reveals abundant novel major lineage of archaea in hypersaline microbial communities. *The ISME Journal*, 6, 81–93.

Oren, A. (2013) Life at high salt concentrations. In: Rosenberg, E., DeLong, E.F., Thompson, F., Lory, S. & Stackebrandt, E. (Eds.) *The prokaryotes. Ecophysiology and biochemistry*, 4th edition. New York: Springer Ltd, pp. 429–440.

Oren, A. & Garrity, G.M. (2021) Valid publication of the names of forty-two phyla of prokaryotes. *International Journal of Systematic and Evolutionary Microbiology*, 71, 005056.

Parab, P., Khandeparker, R., Amberkar, U. & Khodse, V. (2017) Enzymatic saccharification of seaweeds into fermentable sugars by xylanase from marine *Bacillus* sp. strain BT21. *3 Biotech*, 7, 296.

Parks, D.H., Chuvochina, M., Chaumeil, P.A., Rinke, C., Mussig, A.J. & Hugenholtz, P. (2020) A complete domain-to-species taxonomy for Bacteria and Archaea. *Nature Biotechnology*, 38, 1079–1086.

Parks, D.H., Chuvochina, M., Waite, D.W., Rinke, C., Skarshewski, A., Chaumeil, P.A. et al. (2018) A standardized bacterial taxonomy based on genome phylogeny substantially revises the tree of life. *Nature Biotechnology*, 36, 996–1004.

Pfennig, N. & Lippert, K.D. (1966) Über das vitamin B12-bedürfnis phototropher Schwefelbakterien. *Archiv für Mikrobiologie*, 55, 245–256.

Podell, S., Emerson, J.B., Jones, C.M., Ugalde, J.A., Welch, S., Heidelberg, K.B. et al. (2014) Seasonal fluctuations in ionic concentrations drive microbial succession in a hypersaline lake community. *The ISME Journal*, 8, 979–990.

Pruesse, E., Quast, C., Knittel, K., Fuchs, B.M., Ludwig, W., Peplies, J. et al. (2007) SILVA: a comprehensive online resource for quality checked and aligned ribosomal RNA sequence data compatible with ARB. *Nucleic Acids Research*, 35, 7188–7196.

Quast, C., Pruesse, E., Yilmaz, P., Gerken, J., Schweer, T., Yarza, P. et al. (2013) The SILVA ribosomal RNA gene database project: improved data processing and web-based tools. *Nucleic Acids Research*, 41, D590–D596.

Richter, M., Rosselló-Móra, R., Glöckner, F.O. & Peplies, J. (2016) JSpeciesWS: a web server for prokaryotic species circumscription based on pairwise genome comparison. *Bioinformatics*, 32, 929–931.

Rinke, C., Chuvochina, M., Mussig, A.J., Chaumeil, P.A., Davín, A.A., Waite, D.W. et al. (2021) A standardized archaeal taxonomy for the genome taxonomy database. *Nature Microbiology*, 6, 946–959.

Rodriguez-R, L.M. & Konstantinidis, K.T. (2014) Bypassing cultivation to identify bacterial species. *Microbe*, 9, 111–118.

Saccò, M., White, N.E., Harrod, C., Salazar, G., Aguilar, P., Cubillos, C.F. et al. (2021) Salt to conserve: a review on the ecology and preservation of hypersaline ecosystems. *Biological Reviews*, 96, 2828–2850.

Sachs, J., Lafortune, G., Kroll, C., Fuller, G. & Woelm, F. (2022) From crisis to sustainable development: the SDGs as roadmap to 2030 and beyond. *Sustainable Development Report 2022*. Cambridge: Cambridge University Press.

Sáez, M.J. & Lagunas, R. (1976) Determination of intermediary metabolites in yeast. critical examination of the effect of sampling conditions and recommendations for obtaining true levels. *Molecular and Cellular Biochemistry*, 13, 73–78.

Schmieder, R. & Edwards, R. (2011) Quality control and preprocessing of metagenomic datasets. *Bioinformatics*, 27, 863–864.

Selivanova, E.A., Poshvina, D.V., Khlopko, Y.A., Gogoleva, N.E. & Plotnikov, A.O. (2018) Diversity of prokaryotes in planktonic communities of saline Sol-Iletsk lakes (Orenburg Oblast, Russia). *Microbiology*, 87, 569–582.

Sorokin, D.Y., Elcheninov, A.G., Khijniak, T.V., Kolganova, T.V. & Kublanov, I.V. (2022) Selective enrichment on a wide polysaccharide spectrum allowed isolation of novel metabolic and taxonomic groups of haloarchaea from hypersaline lakes. *Frontiers in Microbiology*, 13, 1059347.

Sorokin, D.Y., Khijniak, T.V., Elcheninov, A.G., Toshchakov, S.V., Kostrikina, N.A., Bale, N.J. et al. (2019) *Halococcoides cellulosivorans* gen. nov., sp. nov., an extremely halophilic cellulose-utilizing haloarchaeon from hypersaline lakes. *International Journal of Systematic and Evolutionary Microbiology*, 69, 1327–1335.

Sorokin, D.Y., Messina, E., Smedile, F., La Cono, V., Hallsworth, J.E. & Yakimov, M.M. (2021) Carbohydrate-dependent sulfur respiration in halo(alkali)philic archaea. *Environmental Microbiology*, 23, 3789–3808.

Sorokin, D.Y., Toshchakov, S.V., Kolganova, T.V. & Kublanov, I.V. (2015) Halo(natrono)archaea isolated from hypersaline lakes utilize cellulose and chitin as growth substrates. *Frontiers in Microbiology*, 6, 942.

Sun, H.N., Yu, C.M., Fu, H.H., Wang, P., Fang, Z.G., Zhang, Y.Z. et al. (2021) Diversity of marine 1,3-xylan-utilizing bacteria and characters of their extracellular 1,3-xylanases. *Frontiers in Microbiology*, 12, 721422.

Sutter, J.M., Johnsen, U., Reinhardt, A. & Schönheit, P. (2020) Pentose degradation in archaea: halorhabdus species degrade D-xylose, L-arabinose and D-ribose via bacterial-type pathways. *Extremophiles*, 24, 759–772.

Sutter, J.M., Johnsen, U. & Schönheit, P. (2017) Characterization of a pentonolactonase involved in D-xylose and L-arabinose catabolism in the haloarchaeon *Haloferax volcanii*. *FEMS Microbiology Letters*, 364, fnx140. Available from: https://doi.org/10.1093/femsle/fnx140

Timmis, K. & Ramos, J.L. (2021) The soil crisis: the need to treat as a global health problem and the pivotal role of microbes in prophylaxis and therapy. *Microbial Biotechnology*, 14, 769–797.

Valentine, R.C., Shapiro, B.M. & Stadtman, E.R. (1968) Regulation of glutamine synthetase. XII. Electron microscopy of the enzyme from *Escherichia coli*. *Biochemistry*, 7, 2143–2152.

Wainø, M. & Ingvorsen, K. (2003) Production of β-xylanase and β-xylosidase by the extremely halophilic archaeon *Halorhabdus utahensis*. *Extremophiles*, 7, 87–93.

Werner, J., Ferrer, M., Michel, G., Mann, A.J., Huang, S., Juarez, S. et al. (2014) *Halorhabdus tiamatea*: proteogenomics and glycosidase activity measurements identify the first cultivated euryarchaeon from a deep-sea anoxic brine lake as potential polysaccharide degrader. *Environmental Microbiology*, 16, 2525–2537.

Wurtsbaugh, W., Miller, C., Null, S.E., DeRose, R.J., Wilcock, P., Hahnenberger, M. et al. (2017) Decline of the world's saline lakes. *Nature Geoscience*, 10, 816–821.

Yarza, P., Yilmaz, P., Pruesse, E., Glöckner, F.O., Ludwig, W., Schleifer, K.H. et al. (2014) Uniting the classification of cultured and uncultured bacteria and archaea using 16S rRNA gene sequences. *Nature Reviews. Microbiology*, 12, 635–645.

Zhao, D., Zhang, S., Kumar, S., Zhou, H., Xue, Q., Sun, W. et al. (2022) Comparative genomic insights into the evolution of Halobacteria-associated "*Candidatus* Nanohaloarchaeota". *Msystems*, 7, e00669–e00622.

SUPPORTING INFORMATION

Additional supporting information can be found online in the Supporting Information section at the end of this article.

How to cite this article: La Cono, V., Messina, E., Reva, O., Smedile, F., La Spada, G., Crisafi, F. et al. (2023) Nanohaloarchaea as beneficiaries of xylan degradation by haloarchaea. *Microbial Biotechnology*, 00, 1–20. Available from: https://doi.org/10.1111/1751-7915.14272